Tzu Chi Medical Journal 2024; 36 (2): 152-165

Original Article

Protective effects of Jing-Si-herbal-tea in inflammatory cytokines-induced cell injury on normal human lung fibroblast *via* multiomic platform analysis

Chien-Hao Wang[a], Jai-Sing Yang[b], Chao-Jung Chen[c,d], San-Hua Su[a], Hsin-Yuan Yu[a], Yu-Ning Juan[b], Yu-Jen Chiu[e,f,g], Tsung-Jung Ho[h,i]**

[a]Department of Chinese Medicine, Hualien Tzu Chi Hospital, Buddhist Tzu Chi Medical Foundation, Hualien, Taiwan, [b]Department of Medical Research, China Medical University Hospital, China Medical University, Taichung, Taiwan, [c]Graduate Institute of Integrated Medicine, China Medical University, Taichung, Taiwan, [d]Department of Medical Research, Proteomics Core Laboratory, China Medical University Hospital, Taichung, Taiwan, [e]Division of Plastic and Reconstructive Surgery, Department of Surgery, Taipei Veterans General Hospital, Taipei, Taiwan, [f]Department of Surgery, School of Medicine, National Yang Ming Chiao Tung University, Taipei, Taiwan, [g]Institute of Clinical Medicine, National Yang Ming Chiao Tung University, Taipei, Taiwan, [h]Integration Center of Traditional Chinese and Modern Medicine, Hualien Tzu Chi Hospital, Buddhist Tzu Chi Medical Foundation, Hualien, Taiwan, [i]School of Post-Baccalaureate Chinese Medicine, Tzu Chi University, Hualien, Taiwan

Submission : 24-Oct-2023
Revision : 03-Nov-2023
Acceptance : 23-Nov-2023
Web Publication : 26-Mar-2024

Abstract

Objectives: The protective effects and related mechanisms of Jing-Si herbal tea (JSHT) were investigated in cellular damage mediated by pro-inflammatory cytokines, including interleukin (IL)-1β, IL-6, and tumor necrosis factor-α, on normal human lung fibroblast by multiomic platform analysis. **Materials and Methods:** The *in silico* high-throughput target was analyzed using pharmacophore models by BIOVIA Discovery Studio 2022 with ingenuity pathway analysis software. To assess cell viability, the study utilized the MTT assay technique. In addition, the IncuCyte S3 ZOOM System was implemented for the continuous monitoring of cell confluence of JSHT-treated cytokine-injured HEL 299 cells. Cytokine concentrations were determined using a Quantibody Human Inflammation Array. Gene expression and signaling pathways were determined using next-generation sequencing. **Results:** *In silico* high-throughput target analysis of JSHT revealed ingenuity in canonical pathways and their networks. Glucocorticoid receptor signaling is a potential signaling of JSHT. The results revealed protective effects against the inflammatory cytokines on JSHT-treated HEL 299 cells. Transcriptome and network analyses revealed that induction of helper T lymphocytes, TNFSF12, NFKB1-mediated relaxin signaling, and G-protein coupled receptor signaling play important roles in immune regulatory on JSHT-treated cytokine-injured HEL 299 cells. **Conclusion:** The findings from our research indicate that JSHT holds promise as a therapeutic agent, potentially offering advantageous outcomes in treating virus infections through various mechanisms. Furthermore, the primary bioactive components in JSHT justify extended research in antiviral drug development, especially in the context of addressing coronavirus.

Keywords: *Coronavirus, Cytokines, Lung injury, Multiomic, Protective effects*

Introduction

Toward the close of 2019, a newly identified coronavirus, subsequently termed severe acute respiratory syndrome coronavirus 2 (SARS-CoV-2) was first discovered in clusters of pneumonia of unknown cause. This virus led to a global pandemic, recognized as coronavirus disease 2019 (COVID-19). SARS-CoV-2, the novel coronavirus, is classified within the

***Address for correspondence:** Dr. Yu-Jen Chiu, Division of Plastic and Reconstructive Surgery, Department of Surgery, Taipei Veterans General Hospital, 201, Section 2, Shipai Road, Beitou, Taipei, Taiwan.
E-mail: yjchiu2.md08@nycu.edu.tw
Dr. Tsung-Jung Ho, Integration Center of Traditional Chinese and Modern Medicine, Hualien Tzu Chi Hospital, Buddhist Tzu Chi Medical Foundation, 707 Section 3, Chung-Yang Road, Hualien, Taiwan.
E-mail: tjho@tzuchi.com.tw

How to cite this article: Wang CH, Yang JS, Chen CJ, Su SH, Yu HY, Juan YN, *et al.* Protective effects of Jing-Si-herbal-tea in inflammatory cytokines-induced cell injury on normal human lung fibroblast *via* multiomic platform analysis. Tzu Chi Med J 2024;36(2):152-65.

Supplementary material available online

Access this article online

Quick Response Code:

Website: www.tcmjmed.com

DOI: 10.4103/tcmj.tcmj_267_23

beta-coronavirus subfamily of the *Coronaviridae* family and is a zoonotic infectious disease [1,2]. COVID-19 infection can range from being asymptomatic to causing mild symptoms, including fever and dry cough. In severe cases, it may lead to critical adverse events, including sepsis, acute respiratory distress syndrome (ARDS), or life-threatening pneumonia [3]. Among critically ill patients in the intensive care unit, 90-day mortality was 31%, and higher mortality rates were noted in older, diabetic, and obese patients as well as those with severe ARDS [4,5]. The infection mechanism of SARS-CoV-2 involves the invasion of pulmonary cells through angiotensin-converting enzyme-2 receptor (ACE2) [6]. ACE receptors are widely present in animals, and the variable affinity of ACE receptors expressed across species is the primary factor affecting variances in susceptibility to SARS-CoV-2 infection [7,8]. Studies have reported that SARS-CoV-2 mainly infects the lungs and other organs, such as the kidneys and heart [2,9]. The appearance and severity of symptoms vary according to age and sex and are related to the degree of ACE expression in different organs [10]. An imbalance of immune reactions to SARS-CoV-2 may induce ARDS, sepsis, and other lethal inflammation processes [2,3]. Cytokine storms and over-production lead to poor clinical outcomes and are correlated with an elevated mortality rate [5,11].

Currently, vaccines are the most valuable preventative mechanism against SARS-CoV-2. However, a mutation in the receptor-binding domain of the spike protein of SARS-CoV-2 promotes transmission between different hosts and leads to immune escape [12,13]. Globally, five SARS-CoV-2 variants are designated as variants of concern due to their heightened transmissibility and reduced vaccine efficacy. These include Alpha/B.1.1.7, Beta/B.1.351, Gamma/P. 1, Delta/B.1.617.2, and Omicron/B.1.1.529 [14]. Therefore, adjuvant therapy is required to reduce the replication of SARS-CoV-2 *in vivo* and avoid the occurrence of a cytokine storm [11].

Owing to their widespread historical use for treating a variety of illnesses, exploring the potential therapeutic mechanisms and applications of Chinese herbal medicines forms a strong foundation for clinical research. After the severe acute respiratory syndrome (SARS) outbreak in 2003, many literature reviews and publications on treating SARS using traditional Chinese medicines (TCMs) were published [15,16]. Some studies suggested that combined TCM approaches can reduce mortality and relieve symptoms in SARS patients, although the evidence is lacking due to the low methodological quality of experimental trials [17]. Owing to the structure and gene homology of SARS-CoV and SARS-CoV-2, many compounds have been reported to exert defensive effects against SARS-CoV-2 infection [18].

Jing-Si herbal tea (JSHT) [Figure 1a] is a traditional Chinese medicinal formulation developed by Tzu Chi Hospital in Hualien for combating COVID-19 and regulating immunity. It has received approval from Taiwan's Ministry of Health and Welfare [19,20]. In an early clinical trial, the combination of JSHT with standard therapy enhanced the reverse transcription polymerase chain reaction (RT-PCR) cycle threshold value, reduced C-reactive protein levels, and improved the Brixia score in patients with mild-to-moderate COVID-19. These findings suggest that JSHT may be a promising adjunctive treatment for COVID-19 patients [21]. This research examined the protective impact and associated mechanistic pathways of JSHT in mitigating injury induced by pro-inflammatory cytokines, including tumor necrosis factor (TNF)-α, interleukin (IL)-1β, and IL-6, in normal human pulmonary fibroblast cells (HEL 299). We focused on integrating multiomic results from *in silico* and *in vitro* studies, such as ligand profiler target, ingenuity pathway analysis (IPA), pharmacophore fitting and next-generation sequencing (NGS) analysis. Figure 1b illustrates the design framework and schematic representation of the JSHT study. This paper details the mechanisms and targets of JSHT, which make it a potential protective TCM agent for lung inflammation.

Materials and methods

In silico high-throughput target analysis

In silico high-throughput target analysis was conducted *in silico* using BIOVIA Discovery Studio 2022 (Dassault Systèmes) through the application of pharmacophore models. These models were evaluated considering the intricacies of the proteins prepared and their respective ligands. Subsequently, PharmaDB's database of 16,035 pharmacophore models served as the screening basis for every JSHT component. Furthermore, network analysis target outcomes were acquired using IPA software [22,23].

Chemicals and reagents

JSHT contains *Anisomeles indica* (L.) Kuntze., *Artemisia argyi* H. Levl. et Vant., *Chrysanthemum morifolium* Ramat., *Houttuynia cordata* Thunb., *Ophiopogon japonicus* (L.f.) Ker Gawl., *Perilla frutescens* (L.) Britt., *Platycodon grandiflorum* (Jacq.) A.DC., and *Glycyrrhiza uralensis* Fisch., which were obtained from Tzu Chi Hospital, Hualien, Taiwan [20]. Acetonitrile, methanol, and phosphoric acid of high-performance liquid chromatography (HPLC) grade were sourced from Sinopharm Chemical Reagent Co., Ltd. For the procurement of ultrapure water, the Milli-Q water purification system, supplied by EMD Millipore, was employed. The purity of all JSHT standards was >98%, as determined by HPLC. MTT, calceolarioside A (SMB00246), and Sigma-Aldrich and Merck KGaA were the sources for chlorogenic acid (CA) (C3878), while glycyrrhetic acid (G735000) was acquired from Toronto Research Chemicals based in Toronto, Canada. Life Technologies provided essential cell culture supplies, including Dulbecco's modified Eagle's medium (DMEM), l-glutamine, penicillin G, trypsin-EDTA and fetal bovine serum (FBS).

Analysis employing ultra-high capacity trap mass spectrometry

The JSHT extract was formulated with the following composition: *A. argyi* (6 g), *A. indica* (6 g), *Ophiopogon japonicas* (4 g), *Platycodon grandiflorus* (4 g), *H. cordata* (4 g), *P. frutescens* (2 g), *G. uralensis* (2 g), and *C. morifolium* (0.2 g). The mixture underwent a boiling process (100°C) and agitated on a heated plate with 1000 mL of distilled water for 60 min (Corning® PC-220 Analog Hot Plate/Stirrers, 6795-220). Subsequently, the mixture was concentrated

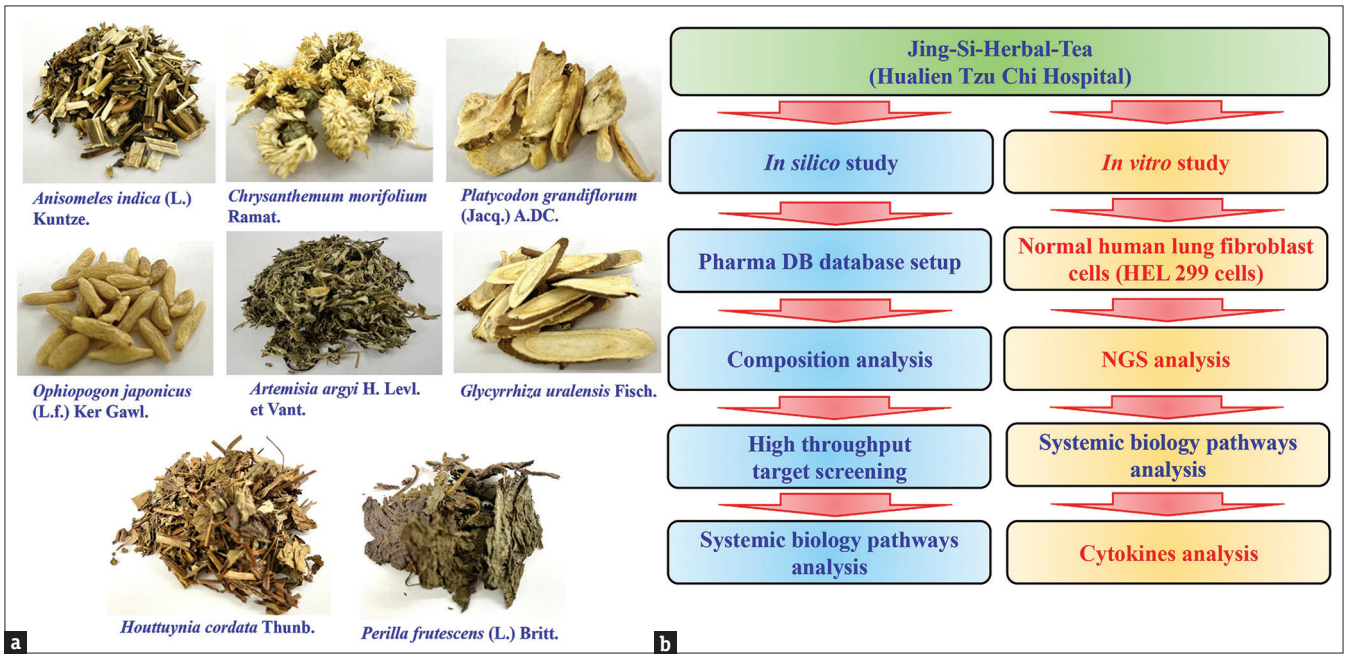

Figure 1: (a) Jing-Si herbal tea (JSHT) formula developed by Hualien Tzu Chi Hospital's efforts in addressing coronavirus disease 2019 infection and modulating immune responses. (b) Study design and JSHT schematics. NGS: Next-generation sequencing

to 3.63 g under reduced pressure employing a rotary evaporator (N-1300VF/OSB-2200; EYELA, Japan) [19]. The chromatographic examination was conducted utilizing the ACQUITY UPLC I-Class/Xevo TQ-XS IVD System, a product of Waters Corporation. This system was equipped with a ZORBAX SB-C18 column, dimensions 4.6 mm × 50 mm, sourced from Agilent Technologies, Inc. Mass spectrometry (MS) data were obtained using an Esquire high capacity trap (HCT) ultra-HCT mass spectrometer (Bruker Daltonics, Bremen, Germany) in the electrospray positive mode. The m/z scan range was 50–1400. MS/MS fragmentation of the five most intense precursors was automatically triggered. The nebulizer gas flow was set at 40 psi, and the drying gas flow rate was adjusted to 10 L/min. The drying temperature was maintained at 350°C. Chromatographic separation was conducted on an Atlantis T3 column (2.1 mm × 150 mm, 3 μm) maintained at 35°C using a binary mobile phase composed of 0.1% formic acid in water (solvent A) and 0.1% formic acid in acetonitrile (solvent B) at the flow rate of 0.25 mL/min following a gradient elution procedure: 0–2 min: 0%–2% solvent B; 2–21 min: 2%–99% solvent B; 21–26 min: 99% solvent B; 26–26.5 min: 99%–100% solvent B; 26.5–30 min: 2% solvent B. The volume injected was 5 μL [23,24].

Cell culture and cell viability

The HEL 299 cell line, a normal human embryonic pulmonary fibroblast variant, was acquired from the Bioresources Collection and Research Center, bearing the catalog number 60117, and was also sourced from the Food Industry Research and Development Institute. The cells were maintained in a 75-T culture flask and cultured in DMEM supplemented with 2 mM L-glutamine, 10% FBS, 100 U/mL penicillin, and 100 μg/mL streptomycin. The culture was incubated at 37°C in a humidified atmosphere with 5% CO_2 [22,23,25]. HEL 299 cells were seeded in 24-well plates at a density of 2.5 × 10^5 cells per milliliter per well. The cells underwent treatment with TNF-α (10 ng/mL), IL-6 (10 ng/mL), IL-1β (10 ng/mL), and JSHT (250, 500, 750, and 1000 μg/mL), calceolarioside A (50–100 μM), CA (50–100 μM), and glycyrrhetic acid (50–100 μM) diluted in 0.1% dimethyl sulfoxide (DMSO) for 12 and/or 24 h. A control treatment was administered to the cells using 0.1% DMSO. Cell viability was assessed using an MTT assay (Sigma) after JSHT treatment for 24 h. The blue MTT formazan crystals were solubilized in DMSO and quantified by measuring absorbance at 570 nm using an enzyme-linked immunosorbent assay reader [24,26].

Real-time cell confluence

The cell confluence assay was performed using the IncuCyte S3 ZOOM System from Essen BioScience. HEL 299 cells were plated at a density of 1 × 10^4 cells per 100 μL per well in a 96-well plate and treated with TNF-α, IL-1β, IL-6 (10 ng/mL each, individually), and/or 1000 μg/mL of JSHT for a duration of 0–24 h. Cells were visualized and photographed every 2 h, as previously described [27].

Inflammatory proteins array detection

The assessment of inflammation-related protein levels was performed using the Quantibody® Human Inflammation Array 3 (QAH-INF-3) from RayBiotech, Inc., located in Norcross, GA, USA. For detection purposes, HEL 299 cells were cultured in 24-well plates at a concentration of 2.5 × 10^5 cells per milliliter per well. The cells were subjected to individual treatments with TNF-α/IL-1β/IL-6 at a concentration of 10 ng/mL each, as well as JSHT at a concentration of 1000 μg/mL, for 24 h. The cells underwent a control treatment with 0.1% DMSO. Cells were harvested, and total proteins were extracted following the manufacturer's instructions

using RIPA buffer (Thermo Fisher Scientific) supplemented with protease inhibitor cocktail (Roche) and phosphatase inhibitor cocktail (Sigma). The protein concentration was quantified using a protein assay kit from Bio-Rad. Fifty microgram samples from individual cells were utilized for the QAH-INF-3 assay. Protein hybridization was conducted following the manufacturer's instructions provided with the QAH-INF-3 kit. Fluorescent images were scanned using an Innopsys innoscan710 (Innopsys, Carbonne, France), and the data were analyzed using Mapix software (Innopsys) [28].

Whole-transcriptome sequencing of next-generation sequencing analysis

To assess the potential mechanisms and signaling pathways of JSHT in HEL 299 cells subjected to cytokine injury induced by TNF-α/IL-1β/IL-6, RNA sequencing analysis of JSHT and cytokine-exposed and cytokine-injured control groups was performed. Total RNA was isolated following the manufacturer's guidelines using TRIzol® reagent (Invitrogen, USA). The purified RNA was quantified at an optical density of 260 nm using an ND-1000 spectrophotometer from Nanodrop Technology, USA. In addition, quantification was performed using a Bioanalyzer 2100 from Agilent Technology, USA, with the RNA 6000 LabChip Kit (Agilent Technology, USA). The preparation of all RNA samples was meticulously conducted in strict accordance with the guidelines set forth in Illumina's established protocol. The construction of the library was carried out using the SureSelect XT HS2 mRNA Library Preparation Kit, sourced from Agilent in the United States. This step was succeeded by a purification process, which involved the employment of AMPure XP beads, a product of Beckman Coulter, also based in the United States. Sequencing was accomplished using Illumina sequencing-by-synthesis technology provided by Illumina, USA (300-cycle paired-end read; 150 PE). Data from sequencing, presented in the FASTQ format, were generated through the application of Illumina's base calling software, bcl2fastq version 2.20. The subsequent steps of adaptor removal and enhancement of sequence quality were proficiently performed using the Trimmomatic tool, version 0.36. The alignment of RNA sequences was performed utilizing HISAT2. For the purpose of normalizing expression levels, the calculation of transcripts per million (TPM) mapped reads was employed. Differential expression analysis was conducted utilizing StringTie (StringTie v2.1.4) and DESeq (DESeq v1.39.0). The detection and correction of genome bias were integrated through the utilization of Welgene Biotech's proprietary pipeline. For statistical analysis, the *P* value computation was based on the hypergeometric distribution, conceptualized as the likelihood of an occurrence in a random selection process [29,30].

Network analysis was conducted using ingenuity pathway analysis

Network analysis was conducted using IPA. Potential compound targets were selected based on a goodness-of-fit value exceeding 0.6. A comprehensive set of 419 human target genes was aggregated as focal entities. These genes were then analyzed utilizing the core analysis functionality embedded in the IPA software (IPA 2021; Qiagen Sciences, Inc.,). This analysis was employed to generate molecular networks derived from the identified targets. Enriched networks, along with their associated ontology groups, upstream regulators, canonical pathways, functions, diseases, and network analysis rankings, were determined based on statistical significance by the Fisher's exact *t*-test ($P < 0.05$). The molecular networks in the QIAGEN knowledge base originated from the focus molecules, with each molecule being interconnected with others in the network. This analysis was performed in duplicate [22,23].

Statistical analysis

The results are expressed as the mean ± standard deviation, and the experiments were conducted independently and in triplicate as indicated. Statistical analysis was carried out using one-way analysis of variance or Tukey's test. Levels of significance were represented with $***P < 0.001$, delineating statistical discrepancies between the control group and the groups treated with TNF-α/IL-1β/IL-6. In contrast, the notation $###P < 0.001$ was used to signify statistical distinctions between the TNF-α/IL-1β/IL-6-treated groups and those treated with JSHT [24,31].

Results

In silico high throughput target analysis of Jing-Si herbal tea

The formulation of JSHT and its constituent herbal elements have been methodically standardized, incorporating a total of eight principal ingredient categories. The key bioactive compounds in JSHT were identified and compiled from the pertinent sections of the 2015 edition of the Chinese Pharmacopoeia [19,20]. The *in silico* high-throughput target was analyzed using pharmacophore models utilizing BIOVIA Discovery Studio 2022 software, provided by Dassault Systèmes, alongside IPA software, facilitated this analysis. The top 20 ingenuity canonical pathways are shown in Figure 2a included glucocorticoid receptor signaling, estrogen receptor signaling, prostate cancer signaling, coronavirus pathogenesis pathway, cardiac hypertrophy signaling (enhanced), molecular cancer mechanisms, hepatic fibrosis signaling pathway, bladder cancer signaling, colorectal cancer metastasis signaling, PI3K/AKT signaling, pancreatic adenocarcinoma signaling, HIF1α signaling, telomerase signaling, IL-17 signaling, endocannabinoid cancer inhibition pathway, regulation of epithelial-mesenchymal transition through the growth factor signaling pathway, PTEN signaling, role of IL-17A in arthritis, leukocyte extravasation signaling, and the senescence pathway. The top 20 ingenuity canonical pathways with their associated molecules are listed in Table 1. These identified targets could be associated with downstream cellular functionalities and phenotypic expressions. A network of associations between JSHT and anti-inflammatory cytokines was generated, and cytokine levels are shown in Figure 2b. The top 20 regulated cytokines included TNF, IFNG, IL1B, IL6, IL4, OSM, IL2, CSF2, IL15, IL13, IL1A, SPP1, CSF1, EPO, CXCL12, PRL, TNFSF11, IL17A, IFNB1, and IL3, which were the most highly regulated by JSHT-targeted genes. Finally, viral infection, lung inflammation, and lower respiratory tract disorder networks were constructed using IPA core analysis. Figure 3 illustrates the focal molecules, depicted in grey,

identified as potential targets of JSHT. The results revealed the potential therapeutic effects of JSHT through interference with pathways related to lung inflammation disease [Figure 3a], lower respiratory tract disorder [Figure 3b], and viral infection [Figure 3c] by identifying JSHT target proteins. Detailed information regarding the target genes is presented in Table 2. The five primary cytokines correlating with these target genes include TNF, IL-1β, IFN-γ, IL-4, and IL-6.

Jing-Si herbal tea treatment revealed protective effects against inflammatory cytokines on HEL 299 cells

We prepared and analyzed JSHT extracts by liquid chromatography. As shown in Figure 4, the UPLC-Q-TOF/MS data showed a standard peak for CA and Glycyrrhetinic acid (GA). Our study explored the putative protective influences of JSHT against cytokine-induced cellular damage in normal human pulmonary HEL 299 cells, employing *in vitro* experimental approaches. Figure 5a demonstrates that cell viability notably diminished in the presence of TNF-α, IL-1β, and IL-6 (10 ng/mL each) in the absence of JSHT extract treatment. In addition, the cellular confluence exhibited a time-dependent alteration, as depicted in Figure 5c. In contrast, groups treated with JSHT showed preserved cellular confluence and protected cell viability. Then, we examined the protective effects of individual phytochemicals, including calceolarioside A, CA, and glycyrrhetic acid. As shown in Figure 5b, cell viability significantly increased after treatment with calceolarioside A or CA (control: 101.07% ± 1.99%; TNF-α/IL-1β/IL-6: 57.39% ± 1.21%; calceolarioside A [100 μM]: 66.17% ± 2.06%; CA [100 μM]: 72.22% ± 2.22%). These results suggest that JSHT and its major components, calceolarioside A and CA, cytoprotective influences in

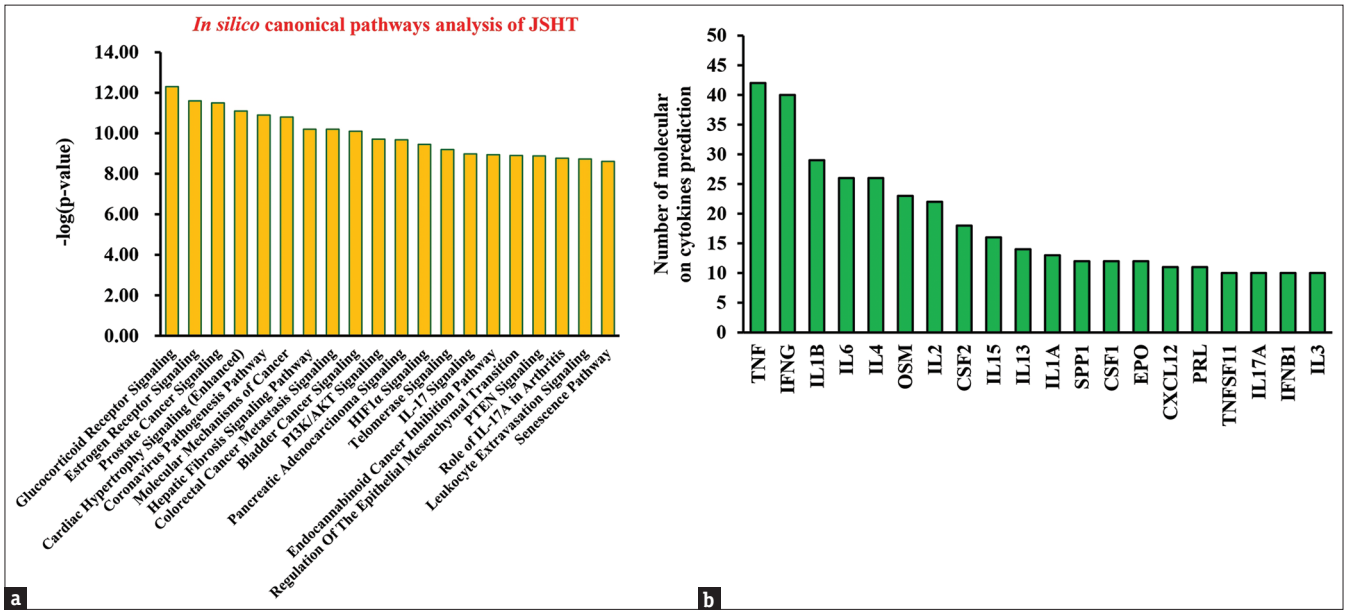

Figure 2: (a) Top 20 ingenuity canonical pathways of Jing-Si herbal tea (JSHT) by *in silico* high throughput target screening analysis. (b) Ingenuity pathway core analysis for potential cytokines gene targets of JSHT. JSHT: Jing-Si herbal tea, IL: Interleukin, TNF: Tumor necrosis factor

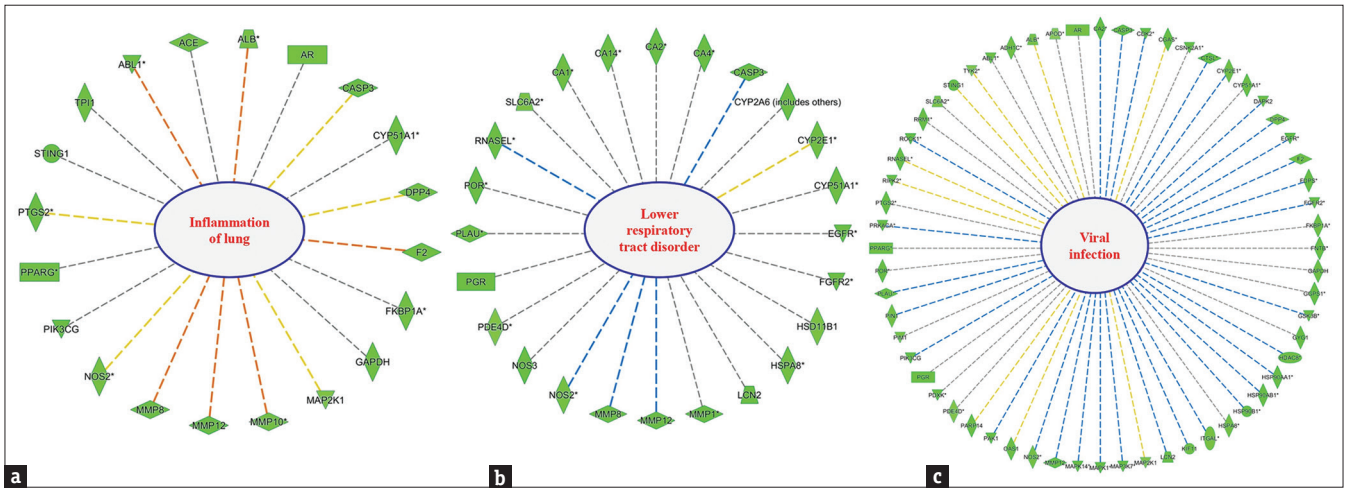

Figure 3: *In silico* pathway core analysis for potential targets of Jing-Si herbal tea in (a) lung inflammation genes; (b) lower respiratory tract disorder; (c) the viral infection genes

Table 1: The top 20 ingenuity canonical pathways of Jing-Si-Herbal-Tea by ingenuity pathway analysis

Ingenuity canonical pathways	*P* (−log)	Ratio	Molecules
Glucocorticoid receptor signaling	12.3	0.0389	AR, EGFR, FBP1, HSP90AA1, HSP90AB1, HSP90B1, HSPA8, MAP2K1, MAP3K7, MAPK1, MAPK10, MAPK14, MMP1, MMP8, NOS2, NOS3, PGR, PIK3CG, PLAU, PPARG, PRKACA, PTGS2, TYK2
Estrogen receptor signaling	11.6	0.0465	EGFR, GSK3B, HSP90AA1, HSP90AB1, HSP90B1, MAP2K1, MAPK1, MMP1, MMP10, MMP12, MMP8, NOS3, PAK1, PGR, PIK3CG, PRKACA, ROCK1, SETD7, TYK2
Prostate cancer signaling	11.5	0.103	ABL1, AR, CDK2, GSK3B, HDAC8, HSP90AA1, HSP90AB1, HSP90B1, MAP2K1, MAPK1, PDPK1, PIK3CG
Cardiac hypertrophy signaling (enhanced)	11.1	0.0382	ACE, ACVR1, FGF1, FGFR2, GSK3B, HDAC8, ITGAL, MAP2K1, MAP3K7, MAPK1, MAPK10, MAPK14, PDE10A, PDE4D, PDE6D, PIK3CG, PRKACA, PTGS2, PTK2, ROCK1, TDP2
Coronavirus pathogenesis pathway	10.9	0.069	ABL1, ACE, AR, CASP3, CDK2, CTSL, HDAC8, MAPK1, MAPK10, MAPK14, OAS1, PTGS2, STING1, TYK2
Molecular mechanisms of cancer	10.8	0.0419	ABL1, AURKA, CASP3, CDK2, CHEK1, CHEK2, GSK3B, HDAC8, ITGAL, MAP2K1, MAP3K7, MAPK1, MAPK10, MAPK14, PAK1, PIK3CG, PRKACA, PTK2, TYK2
Hepatic fibrosis signaling pathway	10.2	0.042	ACVR1, BRD4, CASP3, CSNK1D, CSNK1G3, GSK3B, ITGAL, MAP2K1, MAP3K7, MAPK1, MAPK10, MAPK14, MMP1, PIK3CG, PPARG, PRKACA, PTK2, ROCK1
Colorectal cancer metastasis signaling	10.2	0.0547	CASP3, EGFR, GSK3B, MAP2K1, MAPK1, MAPK10, MMP1, MMP10, MMP12, MMP8, NOS2, PIK3CG, PRKACA, PTGS2, TYK2
Bladder cancer signaling	10.1	0.0948	ABL1, DAPK1, EGFR, FGF1, HDAC8, MAP2K1, MAPK1, MMP1, MMP10, MMP12, MMP8
PI3K/AKT signaling	9.71	0.0637	GSK3B, GYS1, HSP90AA1, HSP90AB1, HSP90B1, ITGAL, MAP2K1, MAPK1, NOS3, PDPK1, PIK3CG, PTGS2, TYK2
Pancreatic adenocarcinoma signaling	9.68	0.0859	ABL1, CDK2, CYP2E1, EGFR, HDAC8, MAP2K1, MAPK1, MAPK10, PIK3CG, PTGS2, TYK2
HIF1α signaling	9.45	0.0607	HIF1AN, HSP90AA1, HSPA8, Ldha/RGD1562690, MAP2K1, MAPK1, MMP1, MMP10, MMP12, MMP8, NOS2, PIK3CG, VHL
Telomerase signaling	9.2	0.0935	ABL1, EGFR, HDAC8, HSP90AA1, HSP90AB1, HSP90B1, MAP2K1, MAPK1, PDPK1, PIK3CG
IL-17 signaling	8.98	0.0635	GSK3B, HSP90AA1, HSP90AB1, HSP90B1, LCN2, MAP3K7, MAPK1, MAPK10, MAPK14, NOS2, PIK3CG, PTGS2
Endocannabinoid cancer inhibition pathway	8.94	0.0733	CASP3, GSK3B, MAP2K1, MAPK1, MAPK14, NOS2, NOS3, PIK3CG, PRKACA, PTK2, ROCK1
Regulation of the epithelial mesenchymal transition by growth factors pathway	8.9	0.0625	EGFR, FGF1, FGFR2, GSK3B, MAP2K1, MAP3K7, MAPK1, MAPK10, MAPK14, MMP1, PIK3CG, TYK2
PTEN signaling	8.88	0.0724	CASP3, CSNK2A1, EGFR, FGFR2, GSK3B, ITGAL, MAP2K1, MAPK1, PDPK1, PIK3CG, PTK2
Role of IL-17A in arthritis	8.77	0.136	MAP2K1, MAPK1, MAPK10, MAPK14, MMP1, NOS2, PIK3CG, PTGS2
Leukocyte extravasation signaling	8.73	0.0603	ABL1, ITGAL, MAPK1, MAPK10, MAPK14, MMP1, MMP10, MMP12, MMP8, PIK3CG, PTK2, ROCK1
Senescence pathway	8.61	0.0464	ACVR1, CDK2, CGAS, CHEK1, CHEK2, DLD, MAP2K1, MAP3K7, MAPK1, MAPK14, PDK2, PIK3CG, STING1, VHL

IL: Interleukin

Table 2: The top 5 inflammatory cytokines regulated gene of Jing-Si-Herbal-Tea by ingenuity pathway analysis analysis

Upstream regulator	Target number	*P*-value of overlap	Target molecule in dataset
TNF	42	9.72E-11	ACE, ALB, AR, BACE1, CA2, CASP3, CDK2, CSF1R, CYP2E1, DPP4, EGFR, FDPS, FGFR2, GSK3B, HSD11B1, HSP90AB1, HSP90B1, HSPA8, ITGAL, LCN2, MAP3K7, MAPK1, MAPK14, MMP1, MMP10, MMP12, MMP8, NOS2, NOS3, OAS1, PARP14, PIK3CG, PIM1, PLAU, PPARG, PTGS2, RIPK2, RRM1, SHBG, TH, TYK2, VDR
IFN-γ	40	1.06E-12	ACE, BACE1, CASP3, CDK2, CGAS, CSF1R, CYP2E1, DAPK1, DPP4, FBP1, FECH, FGF1, FKBP1A, GART, HSP90AA1, HSP90AB1, HSPA8, ITGAL, LCN2, Ldha/RGD1562690, MAP2K1, MAPK14, MMP1, MMP10, MMP12, NOS2, NOS3, OAS1, PARP14, PIM1, PLA2G7, PLAU, PPARG, PTGS2, RIPK2, RORC, SAMHD1, STING1, TPI1, VDR
IL-1β	29	9.11E-10	ACE, BACE1, CASP3, CYP2E1, DPP4, EGFR, FGFR2, GSK3B, GYS1, HSD11B1, LCN2, Ldha/RGD1562690, MAPK14, MMP1, MMP10, MMP12, MMP8, NOS2, NOS3, PAK1, PGR, PIM1, PLAU, PPARG, PTGS2, REN, RIPK2, RORC, VDR
IL-6	26	1.74E-10	ACVR1, ALB, CASP3, CDK2, CHEK1, CSF1R, CYP2E1, DHFR, EGFR, KIF11, LCN2, MAP2K1, MMP1, MMP10, MMP12, MMP8, NOS2, NOS3, PIM1, PLAU, PPARG, PTGS2, RORC, STING1, TH, TYK2
IL-4	26	8.05E-07	CA2, CASP3, CDK2, CSF1R, CTSL, CYP2E1, DPP4, GALK2, HSD11B1, ITGAL, MAP2K1, MAPK1, MMP1, MMP10, MMP12, NOS2, PGK1, PIM1, PIN1, PLAU, PNP, PPARG, PTGS2, SYK, TPI1, VDR

TNF: Tumor necrosis factor, IL: Interleukin

mitigating cytokine-induced injury within HEL 299 cells. Subsequently, we used a protein microarray (Quantibody® Human Inflammation Array) to investigate the inflammatory cytokines in HEL 299 cells. The results revealed that

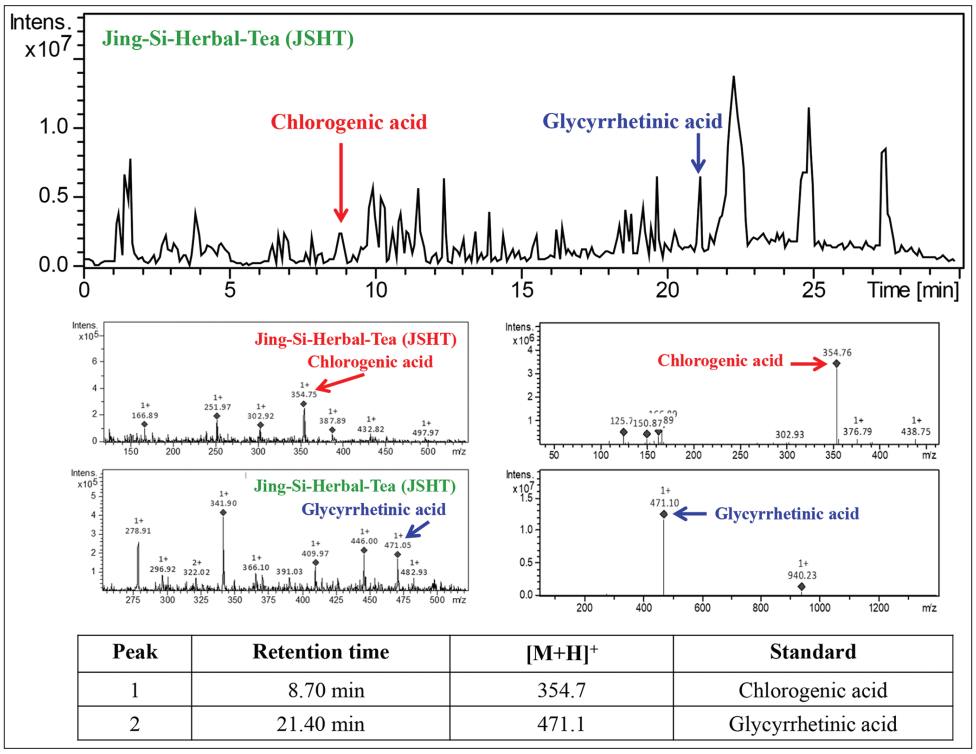

Peak	Retention time	$[M+H]^+$	Standard
1	8.70 min	354.7	Chlorogenic acid
2	21.40 min	471.1	Glycyrrhetinic acid

Figure 4: UPLC-Q-TOF/MS analysis data showing standard peaks of chlorogenic acid and glycyrrhetinic acid. JSHT: Jing-Si herbal tea, CA: Chlorogenic acid, GA: Glycyrrhetinic acid

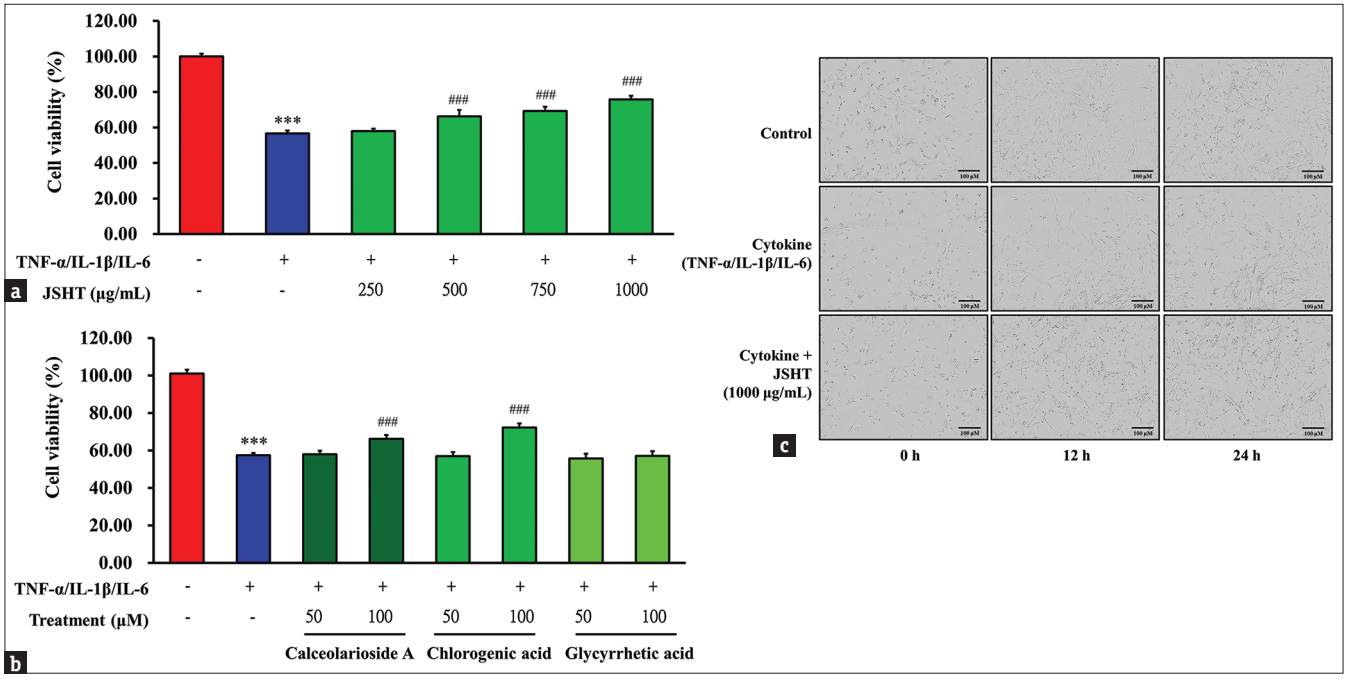

Figure 5: Cell viability exhibited a significant concentration-dependent decrease in the absence of Jing-Si herbal tea (JSHT) extract, calceolarioside A, and chlorogenic acid treatments when exposed to tumor necrosis factor (TNF)-α, interleukin (IL)-1β, and IL-6. (a) HEL 299 cells were seeded at a density of 2.5×10^5 cells/mL/well and subsequently exposed to individual cytokines (TNF-α, IL-1β, and IL-6) at a concentration of 10 ng/mL, along with JSHT at concentrations of 250, 500, 750, and 1000 μg/mL, for a duration of 24 h. (b) The HEL 299 cells were treated with TNF-α/IL-1β/IL-6 (10 ng/mL, individual) and calceolarioside A, chlorogenic acid, glycyrrhetic acid (50–100 μM) for 24 h. The cells were treated with 0.1% DMSO as control treatment. Cell viability was measured by the MTT assay ($n = 3$). The obtained results were subjected to statistical analysis employing a one-way analysis of variance, followed by Tukey's *post hoc* test. Significance levels were denoted as ***$P < 0.001$ and ###$P < 0.001$. (c) Real-time cellular confluence after TNF-α/IL-1β/IL-6 and JSHT treatments changed in a time-dependent manner. JSHT: Jing-Si herbal tea, IL: Interleukin, TNF: Tumor necrosis factor

JSHT (1000 μg/mL) reduced the protein levels of TNF-α, TNF-RI, TNF-RII IL-1α, IL-1β, and IL-6 in cytokine-induced injury in HEL 299 cells [Figure 6]. Based on the results, we treated injured HEL 299 cells with 1000

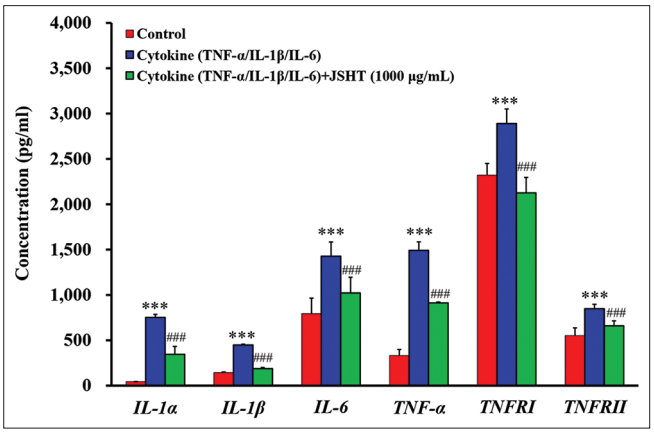

Figure 6: The cytokines concentration of Jing-Si-herbal-tea (JSHT) by protein microarray detection analysis. Cultured HEL 299 cells at a concentration of 2.5×10^5 cells/mL/well were subjected to treatment with individual cytokines, namely tumor necrosis factor-α, interleukin (IL)-1β, and IL-6, each at a concentration of 10 ng/mL, in combination with JSHT at a concentration of 1000 μg/mL. The exposure duration for this experimental setup was 24 h. Cytokines concentration was measured by the protein microarray ($n = 3$). The acquired data were subjected to statistical analysis employing a one-way analysis of variance, followed by *post hoc* testing using Tukey's method. ***$P < 0.001$ and ###$P < 0.001$. JSHT: Jing-Si herbal tea, IL: Interleukin, TNF: Tumor necrosis factor

μg/mL of JSHT to investigate the possible mechanisms and signaling transduction using transcriptome analysis of NGS.

Transcriptome and network analysis

RNA sequencing transcriptional profile analysis was conducted to investigate the mechanism of action (MOA) and signal transduction pathways of JSHT in cytokine-injured HEL 299 cells. The postcytokine-injured samples, JSTH-treated samples, JSTH-treated cytokine-injured samples, and the control group were clustered separately and compared. We compared the differences in the transcriptome of cytokine-injured and JSTH-treated cytokine-injured HEL 299 cells. Figure 7a shows the differential expression in the MA plot. Significantly differentially expressed genes were shown as green dots. Figure 7b shows the differential expression using a volcano plot. Red dots represent genes that are significantly upregulated, while blue dots denote genes that are significantly downregulated. In total, 311 genes were upregulated and 109 genes were downregulated. Supplementary Table 1 shows the raw transcriptome sequencing data of JSHT-treated cytokine-injured HEL 299 cells.

To elucidate the physiological functions of these genes and their related activities, the IPA database was utilized. This was done to examine the protective mechanisms and signaling networks of JSHT in counteracting cytokine-induced cellular injuries. The assessment focused on the rich factor, Q-value, and the quantity of genes enriched in these pathways. Two replicates for normalized RNA sequencing data from cytokine-injured and JSTH-treated cytokine-injured HEL 299 cells were clustered separately using Ingenuity Canonical Pathways in Ingenuity's Knowledge Base. Figure 7c illustrates the pathway analysis and the values of the activation *Z*-score. Following the IPA analysis, a network illustrating the interrelations among various genes was constructed, as depicted in Figure 8a, where induction of helper T lymphocytes, TNFSF12, MYD88, STIRG1, RELA, CREBBP, NFKB1-mediate relaxin signaling, and G-protein coupled receptor signaling played key roles in immune regulatory pathways. The relevant biological pathways of JSTH-treated cytokine-injured HEL 299 cells were analyzed to determine their transcriptional profiles. The predictive target genes and associated pro-inflammatory cytokines in the pulmonary system were analyzed, and the results are shown in Figure 8b. The expression of FGF7, FGF11, FGF17, FGF20, OSM, CD70, LTB, LTA, CD17C, TNFSF11, IL23A, IL23, C8G, and TSLP was decreased and that of AMBP alpha-1-microglobulin/bikunin precursor (ANBP) was increased. Taken together, JSHT treatment of cytokine-injured HEL 299 cells led to decreased cytokine release and inhibited pro-inflammatory processes.

Discussion

Over the past 3 years, although COVID-19 has led to relatively high mortality rates in humans worldwide, with the development of vaccines and the discovery of oral anti-SARS-CoV-2 therapy, fatality rates have begun to decrease gradually. At present, the most significant threat of COVID-19 to human beings is severe infection cytokine storm, resulting in multiorgan failure, which strains the capacities of emergency and hospital services. Further research on antiviral agents and vaccines to prevent the cytokine storm and anti-inflammatory response caused by SARS-CoV-2 remains a major focus in drug discovery and development [2,23]. Clinical evidence has demonstrated that Chinese herbal medicines and/or TCMs may be helpful in preventing or treating human coronavirus-related disorders [2,20,22,23,32]. TCMs have been included in the guidelines for COVID-19 therapies in China. In Taiwan, JSHT has received approval from the Ministry of Health and Welfare, bearing the registration number MOHW-PM-060,635. Furthermore, a drug permit for export purposes has been granted by the same ministry under the registration number CM100106063507. In addition, research papers such as the clinical trial titled "enhances the diminution of SARS-CoV-2 viral load in patients with COVID-19" NCT04967755) have demonstrated potential direct effects of JSHT on disease progression [20]. The combination of JSHT with standard treatment resulted in improvements in the RT-PCR cycle threshold value, C-reactive protein level, and Brixia score among patients with mild-to-moderate COVID-19 symptoms, indicating that JSHT is a promising complementary agent for COVID-19 treatment [21]. Our early review article described the anti-SARS-CoV-2 efficacy and MOA of the active ingredients of JSHT [20]. JSHT includes five herbs with antiviral activity, seven herbs with anti-oxidant activity, and seven herbs with anti-inflammatory activity. In addition, two herbs exert a modulatory effect on the immune system; one herb exhibits anti-thrombotic activity, and one herb has been shown to attenuate cell death [20]. In this study, we used a multiomic platform to analyze the molecular mechanisms of JSHT in the context of inflammatory cytokine-induced cellular injury in human pulmonary HEL 299 cells. Our results from *in silico* [Figures 2 and 3] and *in vitro* studies [Figures 5-8] may provide a useful basis for further clinical studies on the treatment of JSHT. JSHT has been demonstrated to

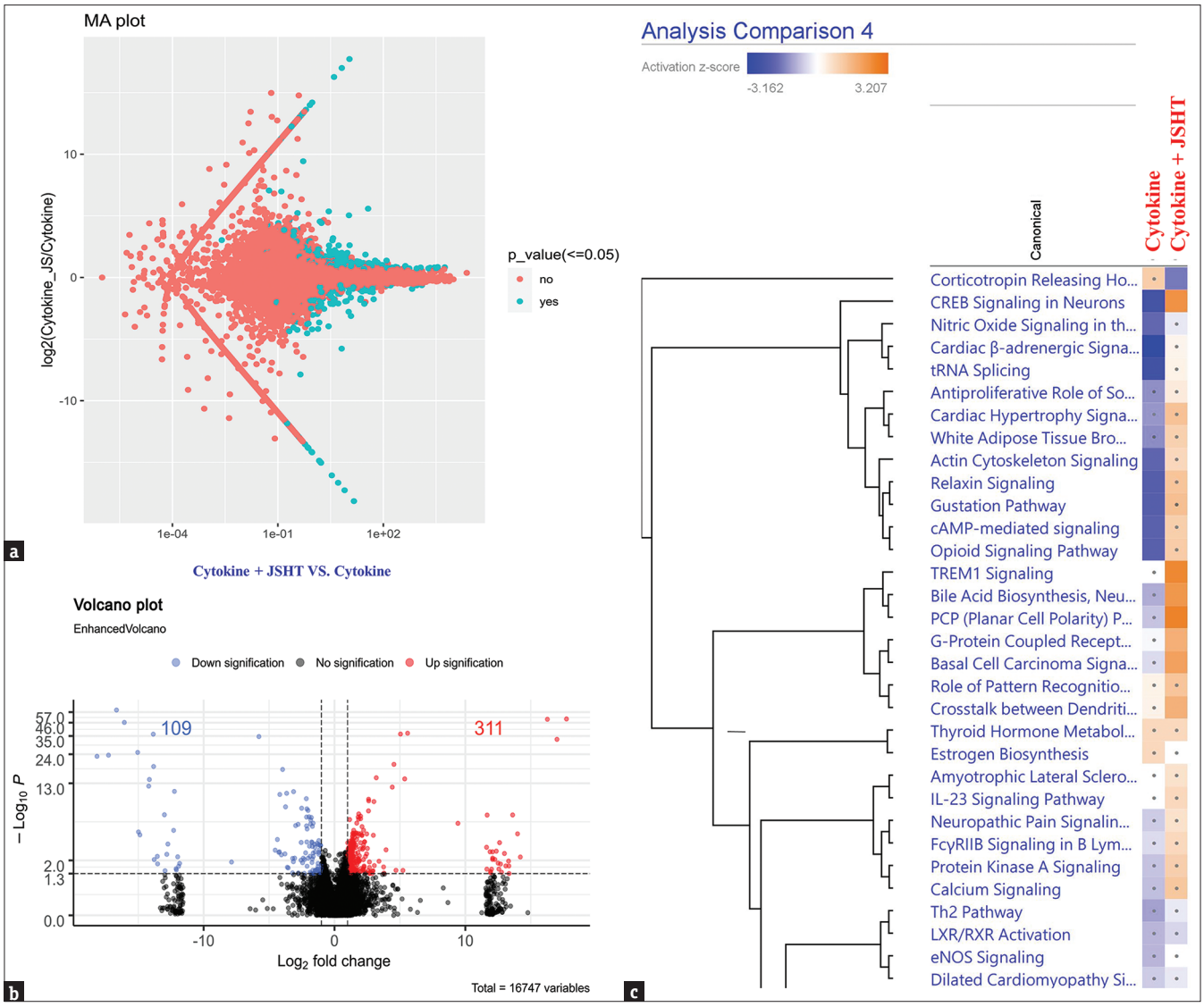

Figure 7: Transcriptome analysis of Jing-Si herbal tea (JSHT)-treated cytokine-injured HEL 299 cells was shown. (a) Differential expression of MA and (b) volcano plots. Cytokine: Tumor necrosis factor -α/interleukin (IL)-1β/IL-6 (10 ng/mL, individual); JSHT. (c) Whole-transcriptome sequencing and comparative analysis using the ingenuity pathway analysis software on JSHT-treated cytokine-injured HEL 299 cells. Blue and red coloring indicates the activation of Z-score values. JSHT: Jing-Si herbal tea, IL: Interleukin

exert pleiotropic effects on aging, skin health, or immune function [19]. The direction of JSHT is adding 300cc water to a bag of herbal tea, boil, and then serve. Therefore, it is most appropriate to conduct research using water extraction. CA and Glycyrrhetinic acid are water soluble compounds, so it is most suitable as a quantitative standard when performing LC-MS/MS analysis [33-35]. In this study, we prepared a water extract of JSHT and analyzed it by UPLC-Q-TOF/MS. Figure 4 illustrates that both positive and negative ion modes were detected, including CA and glycyrrhetinic acid (GA) compounds. Several pharmacological studies have reported the anti-inflammatory and antiviral activities of CA [33-36]. Three approved antiviral drugs (nelfinavir, ritonavir, and lopinavir) showed reliable inhibitory effects in *in silico* and *in vitro* studies on 3CL (pro) main protease [37,38].

In our *in silico* study, additionally, we have demonstrated the inhibitory effect on the 3CL (pro) protease of SARS-CoV-2, though this data is not presented here. Bond interaction analysis showed that CA formed bond interactions with residues CYS145, LEU141, GLY143, HIS41, HIS163, and MET165 of the 3CL (pro) main protease. CA from *C. morifolium* Ramat., has been reported to inhibit the 3CL (pro) main protease on SARS-CoV-2 [39-41]. The pharmacologic activities of CA include modulation of NF-κB activity, TNF signaling pathway, T cells differentiation, and IL-17 function [42,43]. Glycyrrhizic acid (GA) from *G. radix*, which is known as licorice, suppressed LPS-induced TNF-a, IL-1β, nitric oxide, and prostaglandin E2 production through nuclear factor κB (NF-κB) pathway [44,45]. Glycyrrhizic acid (GA) was also reported to bind at the spike glycoprotein receptor-binding domain of the SARS-CoV-2 omicron variant (B.1.1.529) and exhibit high binding affinity with ACE2 [45,46]. Other reports also demonstrated that glycyrrhizic acid (GA) showed highly favorable free binding energies with 3CL (pro) main protease

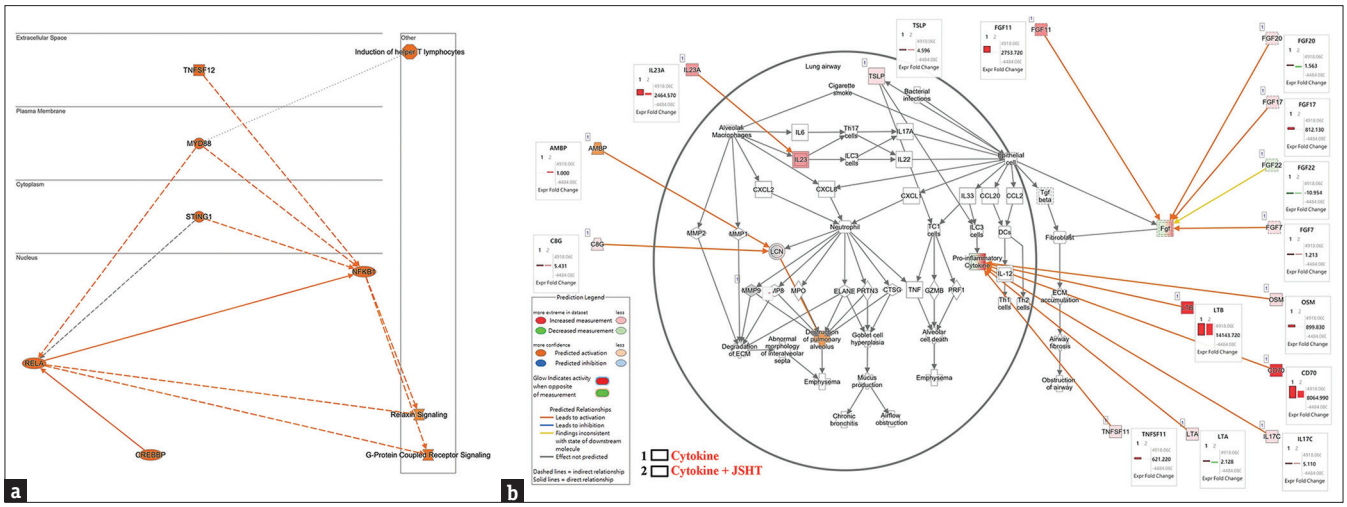

Figure 8: (a) A network depicting associations among various genes was constructed through IPA analysis. Induction of helper T lymphocytes, TNFSF12, MYD88, STIRG1, RELA, CREBBP, NFKB1-mediate relaxin signaling, and G-protein coupled receptor signaling play key roles in immune regulatory pathways. (b) The target genes and associated pro-inflammatory cytokines in the pulmonary system of JSTH-treated cytokine-injured HEL 299 cells were analyzed using IPA software to determine the transcriptional profile. (1: Cytokine (tumor necrosis factor-α/interleukin [IL]-1β/IL-6) treatment; 2: Cytokine with Jing-Si herbal tea treatment. IL: Interleukin, TNF: Tumor necrosis factor

and PLpro [47,48]. Here, bond interaction analysis showed that glycyrrhizic acid (GA) conducted bond interaction with residues CYS145, LEU141, GLY143, HIS41, IS163, and MET165 of 3CL (pro) main protease (data not shown). The binding activity results of glycyrrhizic acid (GA) are similar to those of suggested inhibitors of 3CL (pro) main protease. However, further research on anti-SARS-CoV-2 activity associated with JSHT treatment by *in vitro* and *in vivo* analysis is required.

The advancement of acute pneumonia due to SARS-CoV-2 infection can lead to elevated levels of host lung cell mortality, potentially resulting in diminished lung functionality [3,22]. The inflammatory response, immune system, and various intercellular signaling mechanisms play crucial roles in influencing the progression of COVID-19. Cytokine release syndrome has been associated with poor outcomes of COVID-19, and various conventional and traditional treatment options have been considered to control the cytokine storm [3,22]. Our study focused on the *in vitro* examination of the protective impact of JSHT extract against injury induced by TNF-α, IL-1β, and IL-6 in normal human lung fibroblast cells. The results demonstrated that treating HEL 299 cells with TNF-α/IL-1β/IL-6 (10 ng/mL, individual) decreased cell viability to < 60% compared to the control group [Cell viability: control: 99.73 ± 0.54%; TNF-α/IL-1β/IL-6: 56.62 ± 1.62%, Figure 5a] and induced changes in cellular confluence [Figure 5b]. These results are comparable to those of our early studies, showing that TNF-α/IL-1β/IL-6-induced fibroblast cell damage [22]. In contrast, treatment with JSHT maintained cellular morphology and safeguarded cell viability, achieving approximately 40%–50% of the control group's level in the presence of the three inflammatory cytokines, as shown in Figure 5a. Cell viability significantly increased after treatment with calceolarioside A or CA [Figure 5b]. These results suggest that calceolarioside A and CA play critical roles in protection against lung injury. In previous studies, CA was demonstrated to reduce lipopolysaccharide-induced acute lung injury and protect against Klebsiella pneumoniae infection [49,50].

TCM is thought to comprise a wide array of components, each interacting with diverse targets. We used a multiomic platform (such as high-throughput target analysis, pharmacophore fitting, IPA, and NGS analysis) to investigate the underlying molecular mechanisms responsible for the protective effects of JSHT in inflammatory cytokine-induced cell damage in pulmonary fibroblast cells and anti-SARS-CoV-2 activity. Figure 5 demonstrates the protective effects of JSHT. By NGS analysis, a total of 311 genes exhibited upregulation, while 109 genes were found to be downregulated [Figure 7b]. Helper T lymphocyte induction, TNFSF12, MYD88, STIRG1, RELA, CREBBP, NFKB1-mediate relaxin signaling, and G-protein coupled receptor signaling are major signaling pathways in immune regulatory functions [Figure 8a]. Our results suggest that treatment of JSHT with cytokine-injured HEL 299 cells interferes with the expression of cytokines and pro-inflammatory genes. The innate immune system serves as the initial line of defense against pathogenic organisms [51-54]. Cells constituting the innate immune system, such as neutrophils, monocytes, and macrophages, recognize these pathogens via pattern-recognition receptors and produce cytokines to stimulate the activation of cells within the adaptive immune system [53-55]. IL-1, IL-6, and TNF are pivotal pro-inflammatory cytokines involved in the dynamics of cytokine storms. IL-1 binds to the IL-1 receptor (IL-1R) and activates a cascade of NF-κB pro-inflammatory signaling pathways [56,57]. IL-6, another inflammatory cytokine, binds to the membrane-bound IL-6 receptor (IL-6R) and creates a physiological immune balance. Excessive IL-6 binds to the soluble IL-6 receptor and activates the JAK-STAT3 cascade in endothelial cells, resulting in systemic hyper-inflammation [58-60]. Initial research indicates a correlation between elevated levels of pro-inflammatory cytokines and pulmonary inflammation and lung damage in patients with SARS [61], and many studies have reported that excessive IL-6 levels are highly correlated with mortality

in COVID-19 patients [58-62]. The findings of our study revealed that JSHT potentially reduced the protein levels of IL-1α, IL-1β, IL-6, TNF-α, TNF-RI, and TNF-RII in injury of normal human lung fibroblast cells induced by TNF-α, IL-1β, and IL-6, as illustrated in Figure 6. Based on the results of the *in silico* study, JSHT influences a range of cytokine genes, such as TNF, IFNG, IL1B, IL6, IL4, OSM, IL2, and CSF2, as detailed in Table 2. Notably, all these cytokine genes have been previously identified in patients with COVID-19 [23]. Our NGS and pathway analysis results demonstrated that the induction of helper T lymphocytes, TNFSF12, MYD88, STIRG1, RELA, CREBBP, NFKB1-mediates relaxin signaling, and G-protein coupled receptor signaling plays important roles in immune regulatory pathways in JSHT-treated cytokine-injured HEL 299 cells [Figure 8a]. In addition, the target genes associated with pro-inflammatory cytokines in the pulmonary system were FGF7, FGF11, FGF17, FGF20, OSM, CD70, LTB, LTA, CD17C, TNFSF11, IL23A, IL23, C8G, TSLP, and AMBP [Figure 8b]. NF-κB plays a critical role as a transcription factor, significantly influencing immune functions and inflammatory responses. NF-κB affects cell survival and cell differentiation of immune cells such as T cells, macrophages, dendritic cells, and neutrophils [63]. Severe COVID-19 cases may be characterized by cytokine storms owing to NF-κB, which mediates macrophage activation and inflammatory cytokines production in the lung, ultimately leading organ failure and the development of ARDS [64-66]. Our results suggested that treatment of JSHT with cytokine-injured HEL 299 cells decreases cytokines release and inhibits pro-inflammatory process mediated NF-κB [Figure 8a]. Ovatodiolides in *A. indica* (L.) Kuntze exhibited potent anti-inflammatory properties through an inhibition pathway of TNF-α and IL-12 production [67,68]. *A. argyi* H. *Levl. et Vant.* and its active compound *dehydromatricarin A* were observed to exert potent anti-inflammatory effects in a murine model of acute lung injury [69]. Furthermore, in animal studies conducted on asthmatic subjects, they were shown to decrease inflammatory cell counts and lower the levels of IL-4, IL-5, IL-13, and immunoglobulin E [70].

When pro-inflammatory cytokines such as IL-1 and IL-23 activate macrophages and/or neutrophils, IL-17A is synthesized. IL-17A plays a dual role by contributing to the recruitment of neutrophils and other immune cell types to the infection site, as well as facilitating immune cell infiltration. This, in turn, leads to tissue damage and exacerbates the severity of SARS-CoV-2 infection [71]. The immune responses elicited by SARS-CoV-2 infection lead to the activation and differentiation of T cells, resulting in the production of cytokines commonly associated with various Th17 cell subsets. In addition, infected cells release cytokines as part of the immune response [72]. T-cell immune function against SARS-CoV-2 infection may contribute to clinical protection [71]. Inhibition of IL-17 production reduces the production of pro-inflammatory cytokines IL-1β, TNF, and IL-6 [72]. IL-17 inhibitors have been approved as a successful strategy for reducing psoriasis and psoriatic arthritis injuries [72]. Our NGS analysis results demonstrated that treatment of JSHT with cytokine-injured HEL 299 cells and induction of T help cell signaling play a key role [Figure 8a]. Our high-throughput target analysis results demonstrated that the coronavirus pathogenesis pathway (top 5), IL-17 signaling, and IL-17A signaling are potential targets of JSHT [Figure 2a]. In addition, the top 20 regulated cytokines were regulated most significantly by JSHT-targeted genes [Figure 2b]. Our study indicates that JSHT may serve as a promising multi-target candidate from TCM for the regulation of immune function.

The lungs are vital organs for oxygen and CO_2 exchange. SARS-CoV-2 infects the lungs and causes tissue damage. Severe damage can result in insufficient oxygen exchange and other tissue injuries. Recently, the Warburg effect was shown to exert a significant role in modulating the inflammatory response to COVID-19 [73-75]. SARS-CoV-2-infected pulmonary epithelial cells show increased HIF-1 expression through metabolic reprogramming via the Warburg effect [74]. In addition, these metabolic reprogramming cells increase the consumption of glucose and pro-inflammatory cytokines secretion, including IL-1, IL-6, and TNF-α, and induce monocytes and neutrophils infiltration into the lungs [76,77]. We conducted an *in vitro* investigation to assess the protective effects of JSHT extract against injury induced by TNF-α, IL-1β, and IL-6 in human lung fibroblast cells. Our findings demonstrated that TNF-α, IL-1β, and IL-6-induced injury in pulmonary fibroblast cells. Conversely, treatment with JSHT maintained cellular morphology and safeguarded cell viability in the presence of the three inflammatory cytokines, as depicted in Figure 5. We also demonstrated that JSHT potentially decreased the protein levels of IL-1α, IL-1β, IL-6, TNF-α, TNF-RI, and TNF-RII in TNF-α/IL-1β/IL-6-induced fibroblast cell damage [Figure 6]. The results of the *in silico* analysis showed that a network representing the associations between JSHT and anti-inflammatory cytokines as the Warburg effect pathway included coronavirus pathogenesis pathway, molecular cancer mechanisms, PI3K/AKT signaling, and HIF1α signaling [Figure 2]. These results suggest that JSHT regulates metabolic reprogramming and decreases inflammatory injury induced by cytokines in human pulmonary fibroblasts.

Conclusion

Our findings have unveiled the therapeutic potential of JSHT as a TCM-based agent, which may offer favorable effects to patients with coronavirus through multiple signaling pathways. Furthermore, the primary bioactive compounds found in JSHT merit consideration as promising candidates for subsequent antiviral drug discovery investigations, particularly in the context of coronavirus management. The current investigation relied on bioinformatics and employed an *in silico* approach, necessitating validation through additional experimental analyses.

Data availability statement

All data generated or analyzed during this study are included in this published article (and its supplementary information files).

Acknowledgments

We would like to thank Dharma Master Cheng Yen Shih, Pi-Yu Lin, Shinn-Zong Lin (Hualien Tzu Chi Hospital, Buddhist Tzu Chi Medical Foundation, Hualien), Kuan-Wen Chen, Tzu-Mao Hung (GGA Corporation, Molecular Science and Digital Innovation Center (Taiwan) (WEIGENE BIOTECH CO. LTD, Taiwan), and Mr. Chang-Wei Li (AllBio Science, Inc., Taichung, Taiwan) for their excellent support. Experiments and data analysis were performed in part through the use of the Medical Research Core Facilities Center, Office of Research and Development at China Medical University, Taichung, Taiwan, R.O.C.

Financial support and sponsorship

This work was supported by a grant (IMAR-110-01-26) from the Hualien Tzu Chi Hospital, Buddhist Tzu Chi Medical Foundation, Hualien, Taiwan, to T. J. Ho. This work was also supported by the projects from Dr. Jai-Sing Yang of China Medical University Hospital (DMR-112-135). This study was also supported by the projects from Dr. Yu-Jen Chiu of Taipei Veterans General hospital (V111B-040).

Conflicts of interest

There are no conflicts of interest.

References

1. Cheng YD, Lu CC, Hsu YM, Tsai FJ, Bau DT, Tsai SC, et al. *In silico* and *in vitro* studies of Taiwan Chingguan Yihau (NRICM101) on TNF-α/IL-1β-induced human lung cells. Biomedicine (Taipei) 2022;12:56-71.
2. Tsai SC, Lu CC, Bau DT, Chiu YJ, Yen YT, Hsu YM, et al. Approaches towards fighting the COVID-19 pandemic (Review). Int J Mol Med 2021;47:3-22.
3. Chiu YJ, Chiang JH, Fu CW, Hour MJ, Ha HA, Kuo SC, et al. Analysis of COVID-19 prevention and treatment in Taiwan. Biomedicine (Taipei) 2021;11:1-18.
4. Guan WJ, Ni ZY, Hu Y, Liang WH, Ou CQ, He JX, et al. Clinical characteristics of coronavirus disease 2019 in China. N Engl J Med 2020;382:1708-20.
5. Huang C, Wang Y, Li X, Ren L, Zhao J, Hu Y, et al. Clinical features of patients infected with 2019 novel coronavirus in Wuhan, China. Lancet 2020;395:497-506.
6. Hoffmann M, Kleine-Weber H, Schroeder S, Krüger N, Herrler T, Erichsen S, et al. SARS-CoV-2 cell entry depends on ACE2 and TMPRSS2 and is blocked by a clinically proven protease inhibitor. Cell 2020;181:271-80.e8.
7. Zhao X, Chen D, Szabla R, Zheng M, Li G, Du P, et al. Broad and differential animal angiotensin-converting enzyme 2 receptor usage by SARS-CoV-2. J Virol 2020;94:e00940-20.
8. Shi J, Wen Z, Zhong G, Yang H, Wang C, Huang B, et al. Susceptibility of ferrets, cats, dogs, and other domesticated animals to SARS-coronavirus 2. Science 2020;368:1016-20.
9. Wang MK, Yue HY, Cai J, Zhai YJ, Peng JH, Hui JF, et al. COVID-19 and the digestive system: A comprehensive review. World J Clin Cases 2021;9:3796-813.
10. Li MY, Li L, Zhang Y, Wang XS. Expression of the SARS-CoV-2 cell receptor gene ACE2 in a wide variety of human tissues. Infect Dis Poverty 2020;9:45.
11. Mehta P, McAuley DF, Brown M, Sanchez E, Tattersall RS, Manson JJ, et al. COVID-19: Consider cytokine storm syndromes and immunosuppression. Lancet 2020;395:1033-4.
12. Harvey WT, Carabelli AM, Jackson B, Gupta RK, Thomson EC, Harrison EM, et al. SARS-CoV-2 variants, spike mutations and immune escape. Nat Rev Microbiol 2021;19:409-24.
13. Khateeb J, Li Y, Zhang H. Emerging SARS-CoV-2 variants of concern and potential intervention approaches. Crit Care 2021;25:244.
14. Aleem A, Akbar Samad AB, Slenker AK. Emerging variants of SARS-CoV-2 and novel therapeutics against coronavirus (COVID-19). In: StatPearls. Treasure Island (FL): Copyright © 2022, StatPearls Publishing LLC.; 2022.
15. Yan W, Zheng Y, Zeng X, He B, Cheng W. Structural biology of SARS-CoV-2: Open the door for novel therapies. Signal Transduct Target Ther 2022;7:26.
16. Kim E, Choi J, Min SY, Kim JH, Jeong A. Efficacy of traditional herbal medicine for psychological sequelae in COVID-19 survivors: A protocol for systematic review and meta-analysis. Medicine (Baltimore) 2021;100:e25609.
17. Liu J, Manheimer E, Shi Y, Gluud C. Chinese herbal medicine for severe acute respiratory syndrome: A systematic review and meta-analysis. J Altern Complement Med 2004;10:1041-51.
18. Yang Y, Islam MS, Wang J, Li Y, Chen X. Traditional Chinese medicine in the treatment of patients infected with 2019-new coronavirus (SARS-CoV-2): A review and perspective. Int J Biol Sci 2020;16:1708-17.
19. Shibu MA, Lin YJ, Chiang CY, Lu CY, Goswami D, Sundhar N, et al. Novel anti-aging herbal formulation Jing Si displays pleiotropic effects against aging associated disorders. Biomed Pharmacother 2022;146:112427.
20. Lu P, Tseng C, Lee J, Lee E, Lin Y, Lin I, et al. Jing Si herbal drink as a prospective adjunctive therapy for COVID-19 treatment: Molecular evidence and mechanisms. Pharmacol Res Mod Chin Med 2022;2:100024.
21. Hsieh PC, Chao YC, Tsai KW, Li CH, Tzeng IS, Wu YK, et al. Efficacy and safety of complementary therapy with Jing Si herbal tea in patients with mild-to-moderate COVID-19: A prospective cohort study. Front Nutr 2022;9:832321.
22. Lin C, Tsai FJ, Hsu YM, Ho TJ, Wang GK, Chiu YJ, et al. Study of Baicalin toward COVID-19 treatment: *In silico* target analysis and *in vitro* inhibitory effects on SARS-CoV-2 proteases. Biomed Hub 2021;6:122-37.
23. Huang CW, Ha HA, Tsai SC, Lu CC, Lee CY, Tsai YF, et al. *In silico* target analysis of treatment for COVID-19 using Huang-Lian-Shang-Qing-Wan, a traditional Chinese medicine formula. Nat Prod Commun 2021;16:1934578X211030818.
24. Yang JS, Kang CY, Su CH, Chen CJ, Chiu YJ, Hsu YM. *Helicobacter pylori* targets in AGS human gastric adenocarcinoma: *In situ* proteomic profiling and systematic analysis. Anticancer Res 2022;42:531-46.
25. Huang TY, Peng SF, Huang YP, Tsai CH, Tsai FJ, Huang CY, et al. Combinational treatment of all-trans retinoic acid (ATRA) and bisdemethoxycurcumin (BDMC)-induced apoptosis in liver cancer Hep3B cells. J Food Biochem 2020;44:e13122.
26. Chiu YJ, Yang JS, Tsai FJ, Chiu HY, Juan YN, Lo YH, et al. Curcumin suppresses cell proliferation and triggers apoptosis in vemurafenib-resistant melanoma cells by downregulating the EGFR signaling pathway. Environ Toxicol 2022;37:868-79.
27. Ha HA, Chiang JH, Tsai FJ, Bau DT, Juan YN, Lo YH, et al. Novel quinazolinone MJ-33 induces AKT/mTOR-mediated autophagy-associated apoptosis in 5FU-resistant colorectal cancer cells. Oncol Rep 2021;45:680-92.
28. Wang S, Lu Y, Hong Q, Geng X, Wang X, Zheng W, et al. Protein array-based detection of proteins in kidney tissues from patients with membranous nephropathy. Biomed Res Int 2017;2017:7843584.
29. Chiu YJ, Tsai FJ, Bau DT, Chang LC, Hsieh MT, Lu CC, et al. Next-generation sequencing analysis reveals that MTH-3, a novel curcuminoid derivative, suppresses the invasion of MDA-MB-231 triple-negative breast adenocarcinoma cells. Oncol Rep 2021;46:133.
30. Ha HA, Yang JS, Tsai FJ, Li CW, Cheng YD, Li J, et al. Establishment of a novel temozolomide resistant subline of glioblastoma multiforme cells and comparative transcriptome analysis with parental cells. Anticancer

Res 2021;41:2333-47.
31. Yang JS, Liu TY, Chen YC, Tsai SC, Chiu YJ, Liao CC, et al. Genome-wide association study of alopecia areata in Taiwan: The conflict between individuals and hair follicles. Clin Cosmet Investig Dermatol 2023;16:2597-612.
32. Wang Y, Greenhalgh T, Wardle J, Oxford TCM Rapid Review Team. Chinese herbal medicine ("3 medicines and 3 formulations") for COVID-19: Rapid systematic review and meta-analysis. J Eval Clin Pract 2022;28:13-32.
33. Lin LZ, Harnly JM. Identification of the phenolic components of chrysanthemum flower (*Chrysanthemum morifolium* Ramat). Food Chemistry 2010;120:319-26.
34. Tian D, Yang Y, Yu M, Han ZZ, Wei M, Zhang HW, et al. Anti-inflammatory chemical constituents of flos chrysanthemi indici determined by UPLC-MS/MS integrated with network pharmacology. Food Funct 2020;11:6340-51.
35. Gour A, Manhas D, Bag S, Gorain B, Nandi U. Flavonoids as potential phytotherapeutics to combat cytokine storm in SARS-CoV-2. Phytother Res 2021;35:4258-83.
36. Patil RS, Khatib NA, Patil VS, Suryawanshi SS. Chlorogenic acid may be a potent inhibitor of dimeric SARS-CoV-2 main protease 3CLpro: An *in silico* study. Tradit Med Res 2021;6:14.
37. Aghaee E, Ghodrati M, Ghasemi JB. *In silico* exploration of novel protease inhibitors against coronavirus 2019 (COVID-19). Inform Med Unlocked 2021;23:100516.
38. Barlow A, Landolf KM, Barlow B, Yeung SY, Heavner JJ, Claassen CW, et al. Review of emerging pharmacotherapy for the treatment of coronavirus disease 2019. Pharmacotherapy 2020;40:416-37.
39. Bahun M, Jukić M, Oblak D, Kranjc L, Bajc G, Butala M, et al. Inhibition of the SARS-CoV-2 3CL (pro) main protease by plant polyphenols. Food Chem 2022;373:131594.
40. Wang WX, Zhang YR, Luo SY, Zhang YS, Zhang Y, Tang C. Chlorogenic acid, a natural product as potential inhibitor of COVID-19: Virtual screening experiment based on network pharmacology and molecular docking. Nat Prod Res 2022;36:2580-4.
41. Yu JW, Wang L, Bao LD. Exploring the active compounds of traditional Mongolian medicine in intervention of novel coronavirus (COVID-19) based on molecular docking method. J Funct Foods 2020;71:104016.
42. Su H, Wu G, Zhan L, Xu F, Qian H, Li Y, et al. Exploration of the mechanism of Lianhua Qingwen in treating influenza virus pneumonia and new coronavirus pneumonia with the concept of "different diseases with the same treatment" based on network pharmacology. Evid Based Complement Alternat Med 2022;2022:5536266.
43. Shraibom N, Madaan A, Joshi V, Verma R, Chaudhary A, Mishra G, et al. Evaluation of *in vitro* anti-psoriatic activity of a novel polyherbal formulation by multiparametric analysis. Antiinflamm Antiallergy Agents Med Chem 2017;16:94-111.
44. Wang XR, Hao HG, Chu L. Glycyrrhizin inhibits LPS-induced inflammatory mediator production in endometrial epithelial cells. Microb Pathog 2017;109:110-3.
45. Sun Z, He G, Huang N, Thilakavathy K, Lim JC, Kumar SS, et al. Glycyrrhizic acid: A natural plant ingredient as a drug candidate to treat COVID-19. Front Pharmacol 2021;12:707205.
46. Vardhan S, Sahoo SK. Computational studies on the interaction of SARS-CoV-2 Omicron SGp RBD with human receptor ACE2, limonin and glycyrrhizic acid. Comput Biol Med 2022;144:105367.
47. Mahdian S, Ebrahim-Habibi A, Zarrabi M. Drug repurposing using computational methods to identify therapeutic options for COVID-19. J Diabetes Metab Disord 2020;19:691-9.
48. Vardhan S, Sahoo SK. *In silico* ADMET and molecular docking study on searching potential inhibitors from limonoids and triterpenoids for COVID-19. Comput Biol Med 2020;124:103936.
49. Liu C, Cheng X, Sun J, Zhang S, Zhang Q. Mechanism of chlorogenic acid reducing lipopolysaccharide-induced acute lung injury in mice by regulating miR-223/NLRP3axis. Zhong Nan Da Xue Xue Bao Yi Xue Ban 2022;47:280-8.
50. Tan S, Gao J, Li Q, Guo T, Dong X, Bai X, et al. Synergistic effect of chlorogenic acid and levofloxacin against *Klebsiella* pneumonia infection *in vitro* and *in vivo*. Sci Rep 2020;10:20013.
51. Tomalka JA, Suthar MS, Deeks SG, Sekaly RP. Fighting the SARS-CoV-2 pandemic requires a global approach to understanding the heterogeneity of vaccine responses. Nat Immunol 2022;23:360-70.
52. Zhang S, Wang L, Cheng G. The battle between host and SARS-CoV-2: Innate immunity and viral evasion strategies. Mol Ther 2022;30:1869-84.
53. Gusev E, Sarapultsev A, Solomatina L, Chereshnev V. SARS-CoV-2-specific immune response and the pathogenesis of COVID-19. Int J Mol Sci 2022;23:1716.
54. Duan XQ, Xie H, Chen LM. Interaction between SARS-CoV-2 and host innate immunity. Sichuan Da Xue Xue Bao Yi Xue Ban 2022;53:1-6.
55. Madden EA, Diamond MS. Host cell-intrinsic innate immune recognition of SARS-CoV-2. Curr Opin Virol 2022;52:30-8.
56. Manzanares-Meza LD, Valle-Rios R, Medina-Contreras O. Interleukin-1 receptor-like 2: One receptor, three agonists, and many implications. J Interferon Cytokine Res 2022;42:49-61.
57. Wang Y, Zhu K, Dai R, Li R, Li M, Lv X, et al. Specific interleukin-1 inhibitors, specific interleukin-6 inhibitors, and GM-CSF blockades for COVID-19 (at the edge of sepsis): A systematic review. Front Pharmacol 2021;12:804250.
58. Fajgenbaum DC, June CH. Cytokine storm. N Engl J Med 2020;383:2255-73.
59. Kang S, Tanaka T, Narazaki M, Kishimoto T. Targeting interleukin-6 signaling in clinic. Immunity 2019;50:1007-23.
60. Nasonov E, Samsonov M. The role of interleukin 6 inhibitors in therapy of severe COVID-19. Biomed Pharmacother 2020;131:110698.
61. Wong CK, Lam CW, Wu AK, Ip WK, Lee NL, Chan IH, et al. Plasma inflammatory cytokines and chemokines in severe acute respiratory syndrome. Clin Exp Immunol 2004;136:95-103.
62. Liu T, Zhang J, Yang Y, Ma H, Li Z, Zhang J, et al. The role of interleukin-6 in monitoring severe case of coronavirus disease 2019. EMBO Mol Med 2020;12:e12421.
63. Deng S, Hu B, Shen KP, Xu L. Inflammation, macrophage in cancer progression and Chinese herbal treatment. J Basic Clin Pharm 2012;3:269-72.
64. Xia J, Tang W, Wang J, Lai D, Xu Q, Huang R, et al. SARS-CoV-2 N protein induces acute lung injury in mice via NF-κB activation. Front Immunol 2021;12:791753.
65. Berretta AA, Silveira MA, Cóndor Capcha JM, De Jong D. Propolis and its potential against SARS-CoV-2 infection mechanisms and COVID-19 disease: Running title: Propolis against SARS-CoV-2 infection and COVID-19. Biomed Pharmacother 2020;131:110622.
66. Kim KH, Park YJ, Jang HJ, Lee SJ, Lee S, Yun BS, et al. Rugosic acid A, derived from *Rosa rugosa* thunb., is novel inhibitory agent for NF-κB and IL-6/STAT3 axis in acute lung injury model. Phytother Res 2020;34:3200-10.
67. Rao YK, Fang SH, Hsieh SC, Yeh TH, Tzeng YM. The constituents of *Anisomeles indica* and their anti-inflammatory activities. J Ethnopharmacol 2009;121:292-6.
68. Hsieh SC, Fang SH, Rao YK, Tzeng YM. Inhibition of pro-inflammatory mediators and tumor cell proliferation by *Anisomeles indica* extracts. J Ethnopharmacol 2008;118:65-70.
69. Shin NR, Park SH, Ko JW, Ryu HW, Jeong SH, Kim JC, et al. *Artemisia argyi* attenuates airway inflammation in lipopolysaccharide induced acute lung injury model. Lab Anim Res 2017;33:209-15.
70. Shin NR, Ryu HW, Ko JW, Park SH, Yuk HJ, Kim HJ, et al. *Artemisia argyi* attenuates airway inflammation in ovalbumin-induced asthmatic animals. J Ethnopharmacol 2017;209:108-15.

71. Moss P. The T cell immune response against SARS-CoV-2. Nat Immunol 2022;23:186-93.
72. Zou Y, Meng Z. Literature overview of the IL-17 inhibition from psoriasis to COVID-19. J Inflamm Res 2021;14:5611-8.
73. Yang L, Xiong H, Li X, Li Y, Zhou H, Lin X, et al. Network pharmacology and comparative transcriptome reveals biotargets and mechanisms of curcumol treating lung adenocarcinoma patients with COVID-19. Front Nutr 2022;9:870370.
74. Ferraro E, Germanò M, Mollace R, Mollace V, Malara N. HIF-1, the Warburg effect, and macrophage/microglia polarization potential role in COVID-19 pathogenesis. Oxid Med Cell Longev 2021;2021:8841911.
75. Sukkar SG, Bassetti M. Induction of ketosis as a potential therapeutic option to limit hyperglycemia and prevent cytokine storm in COVID-19. Nutrition 2020;79-80:110967.
76. Al-Kuraishy HM, Al-Gareeb AI, Al-Niemi MS, Alexiou A, Batiha GE. Calprotectin: The link between acute lung injury and gastrointestinal injury in COVID-19: Ban or boon. Curr Protein Pept Sci 2022;23:310-20.
77. Cambier S, Metzemaekers M, de Carvalho AC, Nooyens A, Jacobs C, Vanderbeke L, et al. Atypical response to bacterial coinfection and persistent neutrophilic bronchoalveolar inflammation distinguish critical COVID-19 from influenza. JCI Insight 2022;7:e155055.

Supplementary Table 1: Data of transcriptome sequencing on Jing-Si-Herbal-Tea (JSHT)-treated HEL 299 cells was performed

Gene ID	Gene name	Log2 ratio (Cytokine + JSHT/Cytokine)	*P*
ENSG00000267924	AC139769.2	17.729	2.45E-50
ENSG00000215472	RPL17-C18orf32	17.003	2.22E-33
ENSG00000251537	AC005324.3	16.270	5.10E-50
ENSG00000278621	AC037198.2	14.205	6.20E-03
ENSG00000260342	AC138811.2	13.990	7.98E-05
ENSG00000260121	AC138028.4	13.615	3.68E-07
ENSG00000231369	Z97353.1	13.341	4.96E-02
ENSG00000258608	DNAJC19P9	13.327	2.08E-02
ENSG00000272146	ARF4-AS1	13.303	1.10E-02
ENSG00000225313	AL513327.1	13.094	2.08E-02
ENSG00000271699	SNX29P2	12.988	3.60E-03
ENSG00000260571	BNIP3P5	12.766	4.30E-02
ENSG00000228613	AC141930.1	12.688	1.63E-02
ENSG00000255073	ZFP91-CNTF	12.616	5.34E-04
ENSG00000264577	AC010761.1	12.562	3.01E-02
ENSG00000251246	AL691442.2	12.502	1.45E-02
ENSG00000244414	CFHR1	12.367	2.48E-03
ENSG00000286445	AL355334.2	12.257	8.79E-03
ENSG00000232070	TMEM253	12.087	7.29E-03
ENSG00000233967	AL359715.1	12.083	2.76E-03
ENSG00000233673	ANAPC1P1	12.083	8.75E-03
ENSG00000227942	FRMD8P1	12.008	3.06E-02
ENSG00000234709	UPF3AP3	11.933	4.55E-02
ENSG00000238160	LINC02863	11.924	4.03E-02
ENSG00000125954	CHURC1-FNTB	11.890	2.74E-03
ENSG00000206530	CFAP44	11.668	3.86E-07
ENSG00000117472	TSPAN1	11.643	3.04E-02
ENSG00000268030	AC005253.1	11.623	1.27E-03
ENSG00000196136	SERPINA3	9.434	5.13E-06
ENSG00000257379	AC023509.1	5.586	9.68E-38
ENSG00000266086	AC015813.2	5.364	5.29E-15
ENSG00000135437	RDH5	5.229	3.52E-02
ENSG00000257390	AC023055.1	5.044	3.96E-37
ENSG00000240038	AMY2B	4.699	3.48E-02
ENSG00000273763	AC007318.1	4.544	3.78E-20
ENSG00000257921	AC025165.3	4.416	1.08E-12
ENSG00000188629	ZNF177	3.940	1.98E-03
ENSG00000217289	AC079776.1	3.782	4.76E-02
ENSG00000273148	LINC00653	3.753	2.36E-02
ENSG00000279425	AC092279.2	3.401	1.12E-02
ENSG00000286185	AC242842.3	3.192	2.36E-15
ENSG00000166343	MSS51	3.044	1.99E-02
ENSG00000099974	DDTL	3.012	1.98E-09
ENSG00000277304	AC142086.6	2.967	1.12E-04
ENSG00000279030	AC007336.3	2.947	3.68E-02
ENSG00000255524	NPIPB8	2.898	3.82E-02
ENSG00000250111	AC107982.1	2.881	5.00E-02
ENSG00000239653	PSMD6-AS2	2.741	4.21E-02
ENSG00000269533	AC003002.3	2.685	4.99E-02
ENSG00000261542	AC011978.2	2.674	2.49E-02
ENSG00000232186	TERF1P7	2.670	1.24E-02
ENSG00000171121	KCNMB3	2.656	4.69E-02
ENSG00000213250	RBMS2P1	2.616	1.42E-09

Contd...

Supplementary Table 1: Contd....

Gene ID	Gene name	Log2 ratio (Cytokine + JSHT/Cytokine)	*P*
ENSG00000285053	TBCE	2.604	6.71E-10
ENSG00000205236	AC105052.1	2.597	8.79E-08
ENSG00000254732	AP001931.1	2.571	3.58E-02
ENSG00000272410	AC022384.1	2.515	1.55E-03
ENSG00000250132	AC004803.1	2.461	8.16E-05
ENSG00000284337	AC013271.1	2.457	3.81E-03
ENSG00000099251	HSD17B7P2	2.375	4.28E-02
ENSG00000278897	AC020951.1	2.369	5.67E-03
ENSG00000166455	C16orf46	2.300	4.42E-04
ENSG00000269929	MIRLET7A1HG	2.294	4.66E-04
ENSG00000184206	GOLGA6L4	2.272	2.38E-02
ENSG00000147437	GNRH1	2.261	2.11E-02
ENSG00000264112	AC015813.1	2.223	3.39E-05
ENSG00000272772	AC104109.3	2.221	8.76E-04
ENSG00000215252	GOLGA8B	2.209	1.41E-03
ENSG00000273345	AC104109.4	2.203	9.03E-03
ENSG00000188818	ZDHHC11	2.203	3.11E-02
ENSG00000267059	AC005943.1	2.199	3.38E-02
ENSG00000226361	TERF1P5	2.195	2.89E-02
ENSG00000281183	NPTN-IT1	2.152	1.78E-03
ENSG00000250979	AC022905.1	2.107	1.31E-05
ENSG00000245532	NEAT1	2.104	1.06E-04
ENSG00000135315	CEP162	2.102	1.18E-04
ENSG00000251194	AL133330.1	2.036	2.80E-02
ENSG00000286162	AL162253.2	2.017	3.98E-02
ENSG00000183793	NPIPA5	2.005	7.73E-05
ENSG00000254870	ATP6V1G2-DDX39B	1.996	1.27E-06
ENSG00000152926	ZNF117	1.996	5.60E-07
ENSG00000204778	CBWD4P	1.994	5.45E-04
ENSG00000178397	FAM220A	1.979	1.65E-03
ENSG00000270055	AC127502.2	1.960	3.95E-02
ENSG00000189367	KIAA0408	1.917	1.05E-02
ENSG00000283761	AC118553.2	1.907	5.18E-03
ENSG00000075826	SEC31B	1.882	9.91E-03
ENSG00000223546	LINC00630	1.866	1.19E-02
ENSG00000251562	MALAT1	1.855	2.63E-07
ENSG00000143674	MAP3K21	1.846	8.09E-03
ENSG00000230551	AC021078.1	1.840	1.44E-06
ENSG00000153234	NR4A2	1.835	7.57E-05
ENSG00000165115	KIF27	1.827	9.47E-03
ENSG00000004799	PDK4	1.810	7.39E-07
ENSG00000286104	AC016629.3	1.792	3.08E-03
ENSG00000273018	FAM106A	1.781	1.35E-04
ENSG00000240053	LY6G5B	1.732	1.71E-02
ENSG00000138778	CENPE	1.700	4.81E-06
ENSG00000232593	KANTR	1.700	3.76E-02
ENSG00000250519	AP002784.1	1.695	2.91E-04
ENSG00000279342	AP000866.6	1.689	3.24E-02
ENSG00000229152	ANKRD10-IT1	1.687	2.70E-02
ENSG00000258741	H2AZ2P1	1.681	6.42E-03
ENSG00000196597	ZNF782	1.679	1.43E-02
ENSG00000175265	GOLGA8A	1.666	6.57E-05
ENSG00000259522	AL136295.4	1.657	8.68E-04

Contd...

Supplementary Table 1: Contd....

Gene ID	Gene name	Log2 ratio (Cytokine + JSHT/Cytokine)	*P*
ENSG00000122483	CCDC18	1.644	1.29E-03
ENSG00000259959	AC107068.1	1.639	1.15E-02
ENSG00000162927	PUS10	1.627	8.28E-03
ENSG00000257524	AL157935.2	1.616	6.53E-05
ENSG00000283050	GTF2IP12	1.595	3.37E-02
ENSG00000188611	ASAH2	1.594	3.58E-03
ENSG00000183479	TREX2	1.579	3.43E-02
ENSG00000235770	LINC00607	1.576	4.09E-02
ENSG00000198157	HMGN5	1.570	4.21E-02
ENSG00000268173	AC007192.1	1.548	8.49E-05
ENSG00000139116	KIF21A	1.525	1.46E-02
ENSG00000250067	YJEFN3	1.523	1.89E-04
ENSG00000278662	GOLGA6L10	1.522	3.34E-02
ENSG00000115604	IL18R1	1.503	2.66E-02
ENSG00000233327	USP32P2	1.502	6.40E-04
ENSG00000270069	MIR222HG	1.500	5.77E-04
ENSG00000138587	MNS1	1.492	2.97E-02
ENSG00000107890	ANKRD26	1.484	6.09E-04
ENSG00000146247	PHIP	1.476	9.18E-05
ENSG00000173588	CEP83	1.472	8.99E-04
ENSG00000101745	ANKRD12	1.469	3.42E-05
ENSG00000156876	SASS6	1.459	1.61E-03
ENSG00000230373	GOLGA6L5P	1.454	1.34E-02
ENSG00000280046	AC104581.4	1.453	5.42E-03
ENSG00000223509	AC135983.3	1.451	9.86E-03
ENSG00000197969	VPS13A	1.421	1.66E-03
ENSG00000163535	SGO2	1.416	6.86E-05
ENSG00000120832	MTERF2	1.415	3.18E-02
ENSG00000196247	ZNF107	1.414	3.63E-04
ENSG00000175471	MCTP1	1.412	6.26E-04
ENSG00000003987	MTMR7	1.406	2.20E-02
ENSG00000198707	CEP290	1.400	1.21E-04
ENSG00000066279	ASPM	1.399	3.11E-04
ENSG00000174718	RESF1	1.398	7.27E-05
ENSG00000248124	RRN3P1	1.391	3.24E-02
ENSG00000181619	GPR135	1.389	2.64E-02
ENSG00000113369	ARRDC3	1.386	4.37E-04
ENSG00000177853	ZNF518A	1.385	5.18E-03
ENSG00000263006	ROCK1P1	1.385	2.79E-02
ENSG00000196074	SYCP2	1.382	4.73E-02
ENSG00000197044	ZNF441	1.380	6.23E-03
ENSG00000144674	GOLGA4	1.376	1.48E-04
ENSG00000210151	MT-TS1	1.374	2.80E-03
ENSG00000197837	H4-16	1.374	2.46E-02
ENSG00000254536	AL360181.3	1.365	1.95E-02
ENSG00000173209	AHSA2P	1.365	7.28E-04
ENSG00000152409	JMY	1.360	1.37E-03
ENSG00000224287	MSL3P1	1.360	9.66E-03
ENSG00000196437	ZNF569	1.350	2.65E-03
ENSG00000138182	KIF20B	1.348	2.87E-04
ENSG00000188994	ZNF292	1.341	5.20E-04
ENSG00000189423	USP32P3	1.336	1.26E-02
ENSG00000165813	CCDC186	1.331	8.92E-04

Contd...

Supplementary Table 1: Contd....

Gene ID	Gene name	Log2 ratio (Cytokine + JSHT/Cytokine)	*P*
ENSG00000154874	CCDC144B	1.329	7.57E-04
ENSG00000261490	AC005674.2	1.326	4.31E-02
ENSG00000277701	AC159540.2	1.325	3.51E-03
ENSG00000244754	N4BP2L2	1.316	4.75E-03
ENSG00000189195	BTBD8	1.315	2.02E-02
ENSG00000121621	KIF18A	1.314	1.85E-03
ENSG00000153914	SREK1	1.309	2.01E-03
ENSG00000103995	CEP152	1.308	4.11E-03
ENSG00000089048	ESF1	1.307	4.32E-04
ENSG00000133863	TEX15	1.306	2.69E-02
ENSG00000250299	MRPS31P4	1.296	1.99E-02
ENSG00000196696	PDXDC2P-NPIPB14P	1.293	7.43E-03
ENSG00000267680	ZNF224	1.288	4.77E-03
ENSG00000227671	AL390728.4	1.278	1.29E-03
ENSG00000182263	FIGN	1.272	1.13E-02
ENSG00000274272	AC069281.2	1.271	3.76E-02
ENSG00000166004	CEP295	1.264	2.38E-03
ENSG00000279419	AC004925.1	1.264	2.72E-02
ENSG00000180376	CCDC66	1.263	2.34E-03
ENSG00000196693	ZNF33B	1.256	1.09E-02
ENSG00000162572	SCNN1D	1.254	4.29E-02
ENSG00000256525	POLG2	1.250	3.87E-02
ENSG00000241697	TMEFF1	1.250	5.41E-03
ENSG00000177888	ZBTB41	1.250	8.76E-04
ENSG00000178146	AL672207.1	1.245	2.95E-02
ENSG00000267368	UPK3BL1	1.245	5.00E-02
ENSG00000255717	SNHG1	1.241	1.00E-02
ENSG00000288473	AL669830.2	1.234	1.58E-03
ENSG00000251022	THAP9-AS1	1.231	1.29E-02
ENSG00000114857	NKTR	1.225	6.89E-04
ENSG00000214548	MEG3	1.222	1.24E-03
ENSG00000176597	B3GNT5	1.217	3.57E-02
ENSG00000129534	MIS18BP1	1.215	1.66E-03
ENSG00000197050	ZNF420	1.201	4.53E-03
ENSG00000276550	HERC2P2	1.193	2.96E-03
ENSG00000230453	ANKRD18B	1.191	4.93E-02
ENSG00000187790	FANCM	1.191	3.16E-03
ENSG00000143971	ETAA1	1.189	1.95E-03
ENSG00000173275	ZNF449	1.189	5.44E-03
ENSG00000230630	DNM3OS	1.189	2.01E-02
ENSG00000118482	PHF3	1.187	2.18E-03
ENSG00000080345	RIF1	1.186	2.02E-03
ENSG00000178338	ZNF354B	1.185	2.17E-02
ENSG00000075292	ZNF638	1.182	2.54E-03
ENSG00000273136	NBPF26	1.180	8.68E-03
ENSG00000085224	ATRX	1.175	4.13E-04
ENSG00000171016	PYGO1	1.174	2.21E-02
ENSG00000162601	MYSM1	1.173	2.61E-03
ENSG00000258441	LINC00641	1.172	6.17E-03
ENSG00000197978	GOLGA6L9	1.169	3.42E-02
ENSG00000196081	ZNF724	1.169	1.22E-02
ENSG00000132424	PNISR	1.169	2.27E-03
ENSG00000092140	G2E3	1.166	4.95E-03

Contd...

Supplementary Table 1: Contd....

Gene ID	Gene name	Log2 ratio (Cytokine + JSHT/Cytokine)	*P*
ENSG00000197054	ZNF763	1.164	4.53E-02
ENSG00000134897	BIVM	1.162	1.65E-06
ENSG00000257315	ZBED6	1.159	1.35E-03
ENSG00000139618	BRCA2	1.158	7.82E-03
ENSG00000137135	ARHGEF39	1.143	3.48E-02
ENSG00000230397	SPTLC1P1	1.143	2.14E-02
ENSG00000131127	ZNF141	1.142	3.17E-02
ENSG00000083535	PIBF1	1.139	4.43E-03
ENSG00000254413	CHKB-CPT1B	1.135	4.13E-03
ENSG00000197989	SNHG12	1.134	8.69E-03
ENSG00000228315	GUSBP11	1.134	1.27E-02
ENSG00000236801	RPL24P8	1.134	2.01E-02
ENSG00000082269	FAM135A	1.131	1.07E-02
ENSG00000176055	MBLAC2	1.130	2.14E-02
ENSG00000157741	UBN2	1.129	5.72E-03
ENSG00000146414	SHPRH	1.128	7.65E-03
ENSG00000170396	ZNF804A	1.126	3.65E-03
ENSG00000120798	NR2C1	1.126	8.08E-03
ENSG00000141446	ESCO1	1.125	2.70E-03
ENSG00000127081	ZNF484	1.123	1.03E-02
ENSG00000126777	KTN1	1.120	1.53E-03
ENSG00000122008	POLK	1.119	2.84E-02
ENSG00000261408	TEN1-CDK3	1.117	5.59E-03
ENSG00000023287	RB1CC1	1.114	2.23E-03
ENSG00000188234	AGAP4	1.112	2.66E-02
ENSG00000009694	TENM1	1.110	2.44E-02
ENSG00000139132	FGD4	1.109	2.27E-03
ENSG00000280347	AC000123.3	1.108	3.49E-02
ENSG00000136603	SKIL	1.107	1.46E-02
ENSG00000114120	SLC25A36	1.107	1.98E-02
ENSG00000145777	TSLP	1.107	7.85E-03
ENSG00000163428	LRRC58	1.106	3.01E-03
ENSG00000167635	ZNF146	1.106	3.68E-03
ENSG00000118412	CASP8AP2	1.103	3.13E-03
ENSG00000189057	FAM111B	1.100	9.39E-03
ENSG00000119778	ATAD2B	1.099	1.91E-02
ENSG00000149054	ZNF215	1.098	3.03E-02
ENSG00000100815	TRIP11	1.097	1.27E-03
ENSG00000125351	UPF3B	1.095	6.28E-03
ENSG00000189190	ZNF600	1.095	2.72E-02
ENSG00000138399	FASTKD1	1.092	3.62E-02
ENSG00000117262	GPR89A	1.091	3.96E-03
ENSG00000078177	N4BP2	1.085	1.08E-02
ENSG00000135338	LCA5	1.085	8.36E-03
ENSG00000163611	SPICE1	1.085	2.74E-02
ENSG00000165525	NEMF	1.084	2.30E-03
ENSG00000196757	ZNF700	1.083	1.79E-02
ENSG00000196227	FAM217B	1.080	5.24E-03
ENSG00000102189	EEA1	1.080	3.08E-03
ENSG00000145734	BDP1	1.078	1.80E-03
ENSG00000226102	SEPTIN7P3	1.077	1.98E-02
ENSG00000100592	DAAM1	1.076	9.06E-03
ENSG00000223705	NSUN5P1	1.075	1.49E-02

Contd...

Supplementary Table 1: Contd....

Gene ID	Gene name	Log2 ratio (Cytokine + JSHT/Cytokine)	*P*
ENSG00000169131	ZNF354A	1.073	1.22E-02
ENSG00000139793	MBNL2	1.072	1.12E-02
ENSG00000229419	RALGAPA1P1	1.070	2.30E-02
ENSG00000198046	ZNF667	1.069	2.46E-02
ENSG00000047410	TPR	1.068	3.05E-03
ENSG00000183474	GTF2H2C	1.068	7.58E-03
ENSG00000140285	FGF7	1.067	2.59E-03
ENSG00000182504	CEP97	1.066	5.84E-03
ENSG00000117724	CENPF	1.066	4.42E-03
ENSG00000011405	PIK3C2A	1.066	4.05E-03
ENSG00000163029	SMC6	1.065	4.01E-03
ENSG00000256591	AP003108.2	1.065	2.69E-02
ENSG00000159086	PAXBP1	1.064	6.28E-03
ENSG00000146757	ZNF92	1.063	1.19E-02
ENSG00000116741	RGS2	1.053	1.30E-02
ENSG00000230606	AC092683.1	1.053	3.39E-03
ENSG00000181450	ZNF678	1.047	2.09E-02
ENSG00000163738	MTHFD2L	1.045	2.55E-02
ENSG00000137871	ZNF280D	1.045	7.95E-03
ENSG00000138398	PPIG	1.042	5.01E-03
ENSG00000145241	CENPC	1.042	1.37E-02
ENSG00000198105	ZNF248	1.041	7.98E-03
ENSG00000111860	CEP85L	1.040	7.33E-03
ENSG00000153165	RGPD3	1.040	3.35E-02
ENSG00000182903	ZNF721	1.038	1.64E-03
ENSG00000092208	GEMIN2	1.036	4.29E-02
ENSG00000197121	PGAP1	1.036	2.58E-02
ENSG00000129317	PUS7L	1.034	4.79E-03
ENSG00000179104	TMTC2	1.030	4.01E-02
ENSG00000163848	ZNF148	1.024	2.02E-02
ENSG00000205413	SAMD9	1.021	4.47E-03
ENSG00000133739	LRRCC1	1.021	6.39E-03
ENSG00000198464	ZNF480	1.020	8.07E-03
ENSG00000185246	PRPF39	1.019	1.12E-02
ENSG00000138688	KIAA1109	1.012	1.67E-02
ENSG00000032219	ARID4A	1.011	4.66E-03
ENSG00000127914	AKAP9	1.011	5.53E-04
ENSG00000083097	DOP1A	1.011	3.07E-02
ENSG00000164463	CREBRF	1.009	1.86E-02
ENSG00000151835	SACS	1.008	5.30E-03
ENSG00000135968	GCC2	1.006	7.64E-03
ENSG00000118939	UCHL3	1.005	1.88E-02
ENSG00000115355	CCDC88A	1.004	5.53E-03
ENSG00000113448	PDE4D	1.003	3.13E-02
ENSG00000114796	KLHL24	1.002	4.09E-03
ENSG00000198521	ZNF43	1.000	4.29E-03
ENSG00000213689	TREX1	-1.003	2.04E-02
ENSG00000257511	AC084824.1	-1.012	2.78E-02
ENSG00000270800	RPS10-NUDT3	-1.054	9.04E-04
ENSG00000100311	PDGFB	-1.065	9.15E-04
ENSG00000174977	AC026271.1	-1.081	3.45E-02
ENSG00000286219	NOTCH2NLC	-1.127	4.43E-02
ENSG00000149798	CDC42EP2	-1.133	8.31E-04

Contd...

Supplementary Table 1: Contd....

Gene ID	Gene name	Log2 ratio (Cytokine + JSHT/Cytokine)	*P*
ENSG00000270011	ZNF559-ZNF177	-1.137	4.89E-02
ENSG00000234648	AL162151.2	-1.154	2.01E-03
ENSG00000288534	AP001931.2	-1.192	4.06E-03
ENSG00000260643	AC092718.3	-1.192	3.01E-03
ENSG00000229638	RPL4P4	-1.195	3.60E-04
ENSG00000177272	KCNA3	-1.207	4.11E-02
ENSG00000203761	MSTO2P	-1.224	8.00E-04
ENSG00000131737	KRT34	-1.261	1.51E-02
ENSG00000255339	AL133352.1	-1.263	2.26E-02
ENSG00000254852	NPIPA2	-1.277	3.01E-02
ENSG00000255135	AP002360.1	-1.321	4.14E-02
ENSG00000255526	NEDD8-MDP1	-1.326	3.09E-02
ENSG00000163219	ARHGAP25	-1.329	6.18E-04
ENSG00000229018	PMS2P7	-1.377	3.58E-02
ENSG00000154133	ROBO4	-1.453	3.43E-02
ENSG00000214654	B3GNT10	-1.478	2.84E-03
ENSG00000203995	ZYG11A	-1.479	3.50E-02
ENSG00000215915	ATAD3C	-1.486	1.30E-03
ENSG00000228903	RASA4CP	-1.520	7.36E-04
ENSG00000263887	AC053481.2	-1.612	4.89E-02
ENSG00000166317	SYNPO2L	-1.618	5.74E-03
ENSG00000185839	AL035411.1	-1.626	3.33E-03
ENSG00000213780	GTF2H4	-1.631	4.89E-06
ENSG00000232553	CLK2P1	-1.653	3.45E-02
ENSG00000276345	AC004556.3	-1.687	1.20E-05
ENSG00000006210	CX3CL1	-1.688	8.10E-03
ENSG00000255639	AC005833.1	-1.695	1.09E-03
ENSG00000253767	PCDHGA8	-1.710	5.40E-04
ENSG00000187013	LINC02875	-1.719	1.33E-02
ENSG00000273590	SMIM11B	-1.741	4.62E-04
ENSG00000174028	FAM3C2	-1.766	8.65E-07
ENSG00000023892	DEF6	-1.801	4.87E-02
ENSG00000257949	TEN1	-1.823	1.82E-06
ENSG00000250021	ARPIN-AP3S2	-1.833	6.22E-06
ENSG00000272449	AL139246.5	-1.863	4.30E-02
ENSG00000284391	AL139398.1	-1.866	5.55E-03
ENSG00000234287	AC099560.2	-1.914	1.03E-03
ENSG00000254692	AL136295.1	-1.943	6.96E-07
ENSG00000230667	SETSIP	-2.014	7.33E-03
ENSG00000137411	VARS2	-2.024	7.29E-08
ENSG00000257207	AC112229.3	-2.091	2.42E-05
ENSG00000254806	SYS1-DBNDD2	-2.094	2.15E-02
ENSG00000268575	AL031282.2	-2.110	4.11E-08
ENSG00000268083	AC008982.1	-2.115	4.68E-04
ENSG00000283390	AC068631.3	-2.136	7.54E-07
ENSG00000182890	GLUD2	-2.138	1.05E-05
ENSG00000261553	AL137782.1	-2.155	5.15E-10
ENSG00000203618	GP1BB	-2.207	3.24E-03
ENSG00000256206	AC018523.2	-2.292	8.88E-03
ENSG00000103710	RASL12	-2.309	4.89E-02
ENSG00000272822	AC073610.2	-2.387	7.38E-03
ENSG00000151967	SCHIP1	-2.442	1.38E-02
ENSG00000274810	NPHP3-ACAD11	-2.511	3.16E-08

Contd...

Supplementary Table 1: Contd....

Gene ID	Gene name	Log2 ratio (Cytokine + JSHT/Cytokine)	*P*
ENSG00000188223	AD000671.1	-2.547	5.14E-04
ENSG00000212643	ZRSR2P1	-2.563	9.73E-03
ENSG00000130940	CASZ1	-2.758	4.67E-02
ENSG00000232527	LINC02802	-2.781	6.78E-06
ENSG00000103426	CORO7-PAM16	-2.969	9.74E-06
ENSG00000114786	ABHD14A-ACY1	-3.043	7.33E-03
ENSG00000167774	AC010323.1	-3.127	1.44E-11
ENSG00000267348	GEMIN7-AS1	-3.140	1.20E-02
ENSG00000144834	TAGLN3	-3.198	7.62E-03
ENSG00000214322	CBX1P2	-3.204	4.65E-02
ENSG00000205639	MFSD2B	-3.536	2.63E-02
ENSG00000236546	MYCL-AS1	-3.603	2.45E-02
ENSG00000240764	PCDHGC5	-3.654	3.50E-11
ENSG00000264058	AC073508.2	-3.739	1.83E-08
ENSG00000279504	AD001527.2	-3.785	3.86E-03
ENSG00000239704	CDRT4	-3.964	3.63E-18
ENSG00000285402	AC244230.2	-4.056	4.44E-03
ENSG00000285130	AL358113.1	-4.180	6.37E-11
ENSG00000257341	AL928654.3	-4.210	2.75E-03
ENSG00000215196	BASP1-AS1	-4.252	3.04E-03
ENSG00000172548	NIPAL4	-4.364	2.83E-04
ENSG00000260899	AC106886.2	-4.533	2.11E-03
ENSG00000270181	BIVM-ERCC5	-5.775	2.57E-35
ENSG00000272821	U62317.1	-7.870	1.25E-02
ENSG00000285427	SOD2-OT1	-11.834	1.50E-02
ENSG00000235529	AGAP1-IT1	-11.908	2.16E-02
ENSG00000254968	LINC02763	-11.983	6.02E-03
ENSG00000231050	AL109917.1	-12.082	3.35E-02
ENSG00000205436	EXOC3L4	-12.112	2.91E-02
ENSG00000269693	AC010422.6	-12.234	1.24E-11
ENSG00000260853	AC109460.2	-12.294	3.45E-05
ENSG00000100121	GGTLC2	-12.735	7.01E-04
ENSG00000222032	AC112721.2	-12.817	4.10E-03
ENSG00000265818	EEF1E1-BLOC1S5	-12.951	3.65E-02
ENSG00000273259	AL049839.2	-12.998	3.44E-07
ENSG00000269688	AC008982.2	-13.517	1.60E-02
ENSG00000238123	MID1IP1-AS1	-13.540	5.63E-03
ENSG00000259079	AC005476.1	-13.778	8.95E-03
ENSG00000283765	AC131160.1	-13.824	2.79E-19
ENSG00000285238	AC006064.6	-13.848	5.09E-37
ENSG00000260272	AC093525.2	-14.146	8.14E-15
ENSG00000259171	AL163636.2	-14.195	5.76E-13
ENSG00000251259	AC004069.1	-14.870	1.02E-04
ENSG00000205362	MT1A	-14.982	5.11E-05
ENSG00000256500	AL139300.1	-15.042	1.15E-25
ENSG00000261796	ISY1-RAB43	-16.060	6.13E-47
ENSG00000285991	AL355312.5	-16.658	3.68E-60
ENSG00000235236	AC137630.2	-17.271	2.86E-24
ENSG00000277702	AC239859.5	-18.151	9.91E-24